Illinois State University
ISU ReD: Research and eData

Theses and Dissertations

10-30-2023

Synthesis and Biological Assessment of Alkyl Pyridine Antimicrobials

Juan Canchola
Illinois State University, jcancho@ilstu.edu

Follow this and additional works at: https://ir.library.illinoisstate.edu/etd

Recommended Citation
Canchola, Juan, "Synthesis and Biological Assessment of Alkyl Pyridine Antimicrobials" (2023). *Theses and Dissertations*. 1849.
https://ir.library.illinoisstate.edu/etd/1849

This Thesis is brought to you for free and open access by ISU ReD: Research and eData. It has been accepted for inclusion in Theses and Dissertations by an authorized administrator of ISU ReD: Research and eData. For more information, please contact ISUReD@ilstu.edu.

SYNTHESIS AND BIOLOGICAL ASSESSMENT OF ALKYLPYRIDINE ANTIMICROBIALS

JUAN CANCHOLA

61 Pages

In previous work, my research group and I reported on the synthesis of Anaephenes A and B and confirmed their biological activities. We also found that these compounds were active against drug resistant bacteria such as methicillin-resistant *Staphylococcus aureus* (MRSA). This finding led to a series of structure activity relationship studies (SAR) to develop analogs with improved biological activities. Near the start of my graduate studies, my team and I reported an SAR study where we generated eighteen analogs. Among the series of analogs, we made were a few that displayed high potency and shared a similar amphipathic structure. One of the analogs, a pyridine analogue, was particularly interesting because it exhibited significant biological activities and showed reduced cytotoxicity in a preliminary sheep's blood hemolysis assay.

By employing principles of medicinal chemistry and conducting more SAR studies on the pyridine analog described above, new molecules with improved drug-like properties were designed. Using synthetic methods, five modified pyridine analogs were synthesized and biologically assessed. Several of the alkyl pyridinyls, displayed MIC values that matched the previous lead compounds and retained low levels of toxicity against eukaryotic 3T3 cells. We additionally discovered the unique activity of one of the pyridine analogs (JC-01-074) which was shown to disrupt the cell membrane and displayed bactericidal activity.

Here I provide evidence that this differential biological activity can be attributed to the difference in nitrogen position, yielding different hydrogen bonding and salt forming capabilities. This could disrupt osmotic equilibrium, many other membrane potential based functions, or mechanically perturb the membrane.

KEYWORDS: antibiotics, methicillin-resistant *Staphyloccocsu aureus,* natural products *Staphyloccocsu aureus,* synthesis

SYNTHESIS AND BIOLOGICAL ASSESSMENT OF ALKYLPYRIDINE ANTIMICROBIALS

JUAN CANCHOLA

A Thesis Submitted in Partial
Fulfillment of the Requirements
for the Degree of

MASTER OF SCIENCE

School of Biological Science

ILLINOIS STATE UNIVERSITY

2023

© 2023 Juan Canchola

SYNTHESIS AND BIOLOGICAL ASSESSMENT OF ALKYL PYRIDINE ANTIMICROBIALS

JUAN CANCHOLA

COMMITTEE MEMBERS:

Thomas Hammond, Chair

Martin Engelke

Jan Dahl

Kevin Edwards

ACKNOWLEDGMENTS

While writing this, I am reminiscing on all my experiences, challenges, and fond memories at ISU. A bittersweet sensation fills my heart. To begin, I would like to give a sincere thanks to Dr. Mills. You may not be working in this field anymore and you may never even read this. However, had it not been for you, who knows where I'd be today. I was a confused and lost kid, first generation college student. I had no one to go to for help at home. My parents didn't get to go to high school and my siblings rejected the concept of college education, "we're Mexican, we just aren't good at that kind of stuff" they'd tell me. I had no vision, motivation, nor guidance. I was on the verge of dropping out, but then you accepted me into your lab and showed me how exciting and fulfilling research can be. It was there where I met David Kukla, a good friend, colleague, and mentor. You two showed me that STEM research doesn't have to be painful, boring and it's not something exclusively for "smart people" it can actually be really cool. Moreover, you showed me that succeeding in a difficult field is something anyone can do, I felt included and empowered. Fast forward to today and I have landed an incredible job and for once I am beyond excited for the future. I sincerely don't think this would be the case had you not invited me to work in your lab that day. Another colleague from the Mills lab I'd Like to thank is Emmanuel Ayim, a very dear friend of mine who worked hard to help me finish the synthesis and spectra for some of the important molecules in this study. Near the start of my second semester in graduate school, Dr. Mills quit academia to pursue a career in a different field. I was stranded with a half-completed thesis, no lab and no mentor. That was when I met Dr. Hammond, he accepted me into his lab with open arms.

His incredibly kind and compassionate personality made me feel immediately comfortable in his lab. Dr. Hammond has what I consider the best approach to mentoring. He teaches everything you need to know to get started, doesn't micromanage, then rewards you with trust in the lab. If something came up, he was always there with a quick solution. In Dr. Hammond's lab I was able to acquire new skills and complete my master's project. So, I want to give a huge thanks to Dr. Hammond. Thank you for allowing me in your lab and mentoring me, you are one of the kindest and most caring professionals I have met. I will always say this, Dr. Hammond is one of ISU's most valuable assets. Another mentor I want to give a huge thanks to is Dr. Jeff Helms. Thank you for always giving me career advice and guidance. Your mentorship played a huge role in landing my current job.

I'd also like to thank my committee for all the support. Dr. Engelke, you consistently contacted me to make sure I was on track and always offered to assist and review my work, thank you for that. Dr. Edwards, you generously agreed to join my committee with short notice. Your input and expertise were crucial for my thesis project. I'd also like to thank Dr. Dahl, you encouraged me to get out of my shell and speak with more emotion and enthusiasm. I will always remember when you told me I need to be able to "talk about crap and sell it like its gold!". At first, that didn't really mean much to me. But after job searching and networking, I soon realized how much better everything is when you open up a little.

Lastly, I'd like to thank my friends and family for all the love and support. Diego you were always there when I needed to chat and unwind. Thanks for being such a great friend. Thanks to my parents, maybe you couldn't give me academic advice, but your love and support was more than enough.

Dad, *apa*, you always dreamed of going to school as a young kid on the farm in Mexico. You didn't get a chance to do that, but you are the smartest person I've ever met. You're the reason I did not waiver under adversity nor severe stress. Me and you are alike. We are strong, we are businessmen, intellectuals, natural born entrepreneurs, and true scientist by spirit. School or no school we never give, we were meant for great things, y mas que nada… sabemos que si se puede!

J.C

CONTENTS

TABLES

FIGURES

CHAPTER I: SYNTEHSIS OF THE ANAEPHENE ANTIBIOTICS

Summary

Antibiotic resistance is becoming a major global issue, forcing us to question the stability of our pathogenic defenses. Natural products play a critical role in the development of new antibiotics and provide molecular templates for developing novel classes. Anaephenes A, B, and C are a series of alkylphenols, that have been shown to be effective antibiotics against *Bacillus cereus* and *S. aureus*. Previously, my team and I reported the syntheses of anaephenes A and B and confirmed their biological activities. To expand on these previous efforts, we generated a library of 18 analogs via structure-activity relationships studies (1). These analogs were designed to explore the biological impact of structural variations in the alkyl chain and on the phenol moiety. These studies generated compound 4, which was 4-fold more potent than the natural product (**2**) against MRSA (2 vs. 8 μg/ml) and a pyridine analog (**18**) with an MIC matching that of the natural product (**2**), but with a significant reduction in hemolytic activity (<1% vs. 80% at 100 μM) (1).

Introduction

According to the Centers for Disease Control and Prevention (CDC), about 2.9 million antibiotic-resistant infections occur in the United States each year, resulting in 35,900 deaths (2). Scientists also predict that, if not quickly addressed, by the year 2050, the death rate due to antimicrobial resistance could rise to over 10 million per year (3). With these frightening statistics in mind, it is evident that we need to focus on the development of new therapeutics for the treatment of bacterial infections. Considering that most of the drugs in our clinical pipeline are derivatives of existing antibiotics, they are only short-term solutions and will quickly lose their efficacy (4).

The threat of antibiotic resistance is worsened by the decrease in pharmaceutical interest due to the low profitability of antibiotic drug development, where cancer drugs are highly profitable (5). The responsibility lies on scientists and researchers in academia around the world to work on antibiotics drug discovery research to advance and bring attention to the replenishment of our antibiotic arsenal to fight off the rise of deadly multi-drug resistant bacterial infections.

To develop new antibiotics, more innovative and therapeutic strategies will be required. Natural products are chemicals that are found in nature, they are produced by microorganisms and sessile organisms. Natural products are an optimal avenue for antibiotic discovery because of the vast chemo diversity and various mechanisms of action (6). Anaephenes A (**1**) and B (**2**) are a series of alkylphenol natural products, isolated from a marine cyanobacterium off the coast of Guam, known as *Hormoscilla oscillatoriales* (7). In previous work we found that anaephenes A (**1**) and B (**2**) displayed antimicrobial activity against methicillin-resistant *Staphylococcus aureus* (MRSA), with minimum inhibitory concertation (MIC) values of 16 and 8 μg/mL respectively (Figure 1). These potent antimicrobial activities warranted further investigation, as antibiotics are often developed from natural product antimicrobials (6).

Structure-activity relationship (SAR) studies can be used to identify correlations between the chemical structure of a compound and its biological activity. SAR studies can identify what functional group or structural variation is important for a compound's biological activity. With SAR studies, one can simultaneously collect information on antimicrobial activity and biological target while generating analogs with improved potency and drug-like properties. Some SAR studies use minimum inhibitory concentration (MIC) assays. MIC assays allow the determination

of the minimum concentration of compound required to inhibit bacterial growth, providing an indicator of potency against the strain used. Researchers can then use this information, along with the principles of medicinal chemistry, to design additional analogs with improved activities and properties. It is important to include principles of medicinal chemistry when designing analogs because MIC assays only serve as an indicator of potency, not of drug-like properties. For any lead compound or potential drug candidate, it is critical for researchers to design it to retain efficacy in vivo. A medicinal chemist must consider properties that might impact pharmacokinetic processes such as adsorption, distribution, metabolism, and elimination and avoid off-target binding (8). Certain concepts in medicinal chemistry can be relied on for guidance during drug design. Examples include Lipinski's rules, which guide the selection and design of molecules that are likely to have adequate absorption into the bloodstream, as well as membrane permeability (8).

Concepts of medicinal chemistry were utilized to design a variety of Anaephene A and Anaephene B analogs, synthesis described in Kukla et al 2021. The strategy for designing the analogs was to develop analogs that would give us more information on the moieties structural features that comprise Anaephenes A and B and how they affect antimicrobial activity. To do this, we analyzed the key moieties and structures of the natural products individually. First, we generated analogs with varying degrees of saturation in the alkyl chain (Figure 2). Next, we made analogs with the hydroxy orientated meta (**4**), para (**3**), and ortho (**8**) to the alkyl chain to see if there is an optimal or preferred orientation (Figure 3). Next, we looked at carbon chain length, we made analogues with chain lengths ranging from 3 to 11 carbons after the internal alkyne (Figure 4). The analogs generated in this study were examined to determine the MIC, MBC, and antihemolytic properties to identify an optimal molecular template and better design

more analogs with improved antimicrobial properties.

Materials and Methods

General Experimental Procedures

1H and 13C NMR spectra were obtained on a Bruker 400 MHz Avance III spectrometer or Bruker 500 MHz Avance III spectrometer in CDCl3 unless otherwise noted. Chemical shifts are reported with the residual solvent peak used as an internal standard (CDCl3 = 7.26 ppm for 1H and 77.15 ppm for 13C). High-resolution mass spectra were obtained using positive mode electrospray ionization (ESI+) on a Thermo Scientific Q Exactive hybrid quadripole-Orbitrap mass spectrometer. Analytical HPLC was performed with a Thermo Finnigan Surveyor HPLC utilizing a Thermo Scientific Hypersil GOLD column (5 μm, 100 mm × 4.6 mm) run with 80% methanol and 20% 1.0 M acetic acid as the mobile phase at 1.0 mL/min. Reactions were monitored by TLC analysis (silica gel 60 F254, 250 mm layer thickness) and visualized with a 254 nm UV light. Flash chromatography on SiO2 was used to purify the crude reaction mixtures and performed on a flash system utilizing pre-packed cartridges and linear gradients. All starting materials and solvents were purchased from a commercial chemical company and used as received.

General Synthetic procedure

They key synthetic step for generating all the analogues was a sonagashira cross-coupling reaction, which allows us to attach an alkyl chain to a phenolic head generating the key moiety of all of our analogues. The reaction links terminal alkynes to vinyl halides by forming a carbon-carbon bond, we have previously established this reaction as a route for generating Anaepehenes A and B (1). The General Synthetic procedure (sonagashira cross-coupling reaction): To a solution of tert-butyl(3-iodophenoxy) dimethylsilane (1 eq) in MeCN (0.2 M) was added

terminal alkyne (3 eq) followed by CuI (0.2 eq) and PdCl2(PPh3)2 (0.05 eq). Then triethylamine (3 eq) was added, and the reaction was heated at 60 °C for 2 hours. Then the reaction was cooled to room temperature and tetrabutylammonium fluoride (TBAF) (3 eq) was added. The reaction was stirred at room temperature overnight and then sat. NH4Cl was added. The aqueous layer was extracted with EtOAc (3x), the combined organic layers were then washed with brine, dried (MgSO4), filtered and concentrated under reduced pressure. The residue was purified by flash column chromatography (10-30% EtOAc:Hex) to afford the desired compounds. We followed with work up and other small modification reactions, reported in Kuka et al 2021, to generate all of the analogues in this study (1).

Antibacterial Assays

Minimum inhibitory concentrations (MIC) were determined by broth micro-dilution according to CLSI guidelines (CLSI, 2014). The test medium was lysogeny broth (LB). *S. aureus* (ATCC 25923), MRSA (ATCC 33591), MRSA (ATCC BAA-44), *S. epidermidis* (ATCC 12228), *S. epidermidis* (ATCC 51625), *E. faecalis* (ATCC 29212), *E. faecalis* (ATCC 51299), P. aeruginosa (ATCC 27853), and *A. baumannii* (ATCC 19606) were grown in LB for 6–8 h. These cultures were used to inoculate fresh LB medium at 5×10^5 CFU/mL. The resulting bacterial suspensions were aliquoted (1 mL). To the first row of a 96 well plate was added bacterial stock and compound from a 10 mM DMSO stock to achieve a starting concentration of 128 μg/mL, which was then serially diluted to achieve a concentration of 0 μg/mL at the bottom row. Linezolid (from a 10 mM DMSO stock) was used as a positive control with final concentrations ranging from 0.063 to 128 μg/mL. Inoculated media not treated with compound served as a negative control. The plates were incubated under stationary conditions at 37 °C. After 16 h, minimum inhibitory concentration (MIC) values were recorded as the lowest concentration of

compound at which no visible growth of bacteria was observed, based on duplicate plates performed in three separate experiments. To determine the minimum bactericidal concentration (MBC), 100 μL of culture from wells containing no growth were plated onto tryptic soy agar and incubated at 37 °C overnight. The highest dilution that resulted in 99.9% reduction in the cell count was recorded as the MBC. The MBC values were determined in triplicate.

Hemolytic Activity

Hemolysis assays were performed on mechanically defibrinated sheep blood (Hemostat Labs: DSB50). Defibrinated blood (1.5 mL) was placed into a microcentrifuge tube and centrifuged for 10 min at 10,000 rpm. The supernatant was then removed and then the cells were resuspended in 1 mL of phosphate-buffered saline (PBS). The suspension was centrifuged, the supernatant was removed, and cells were re-suspended two additional times. The final cell suspension was then diluted 10-fold. Test compound solutions were made in PBS and then added to aliquots of the 10-fold suspension dilution of blood. PBS was used as a negative control and a zero-hemolysis marker. Triton X (a 1% sample) was used as a positive control serving as the 100% lysis marker. Samples were then placed in an incubator at 37 °C while being shaken at 200 rpm for one hour. After one hour, the samples were transferred to microcentrifuge tubes and centrifuged for 10 min at 10,000 rpm. The resulting supernatant was diluted by a factor of four in distilled water. The absorbance of the supernatant UV spectrometer at a 540 nm wavelength.

Results

SAR studies and antimicrobial activity of the anaephene analogs

To investigate the significance of Anaephene chemical structure and biological activity, a series of eighteen analogs of Anapehene A and B were synthesized and tested for biological activities against clinically relevant bacteria such as *S. aureus*, methicillin-resistant *S. aureus* and

gram-negative *P. aeruginosa* and *A. baumannii*. The first round of analogs was generated to explore unsaturation levels (Figure 2, Analogs **4**, **6** and **7**). The analog with the internal alkyne and no additional unsaturation was the most potent (Figure 2, Analog **4**). Next, the hydroxy position was investigated. We found that the para/meta positions are equally preferred while ortho reduces potency (Figure 3; Compare analogs **4** and **3** to **9**). Next, we looked at carbon chain length, we made analogs with chain lengths ranging from 3 to 11 carbons after the internal alkyne. We found that analogs with 6–7 carbons after the internal alkyne were the most potent against MSSA, while analogs with 7–10 carbons after the internal alkyne were the most potent against MRSA. We also examined a nitrogen-containing analog of Analog **4**. Specifically, although we found that Analog **4** is two-fold more potent than the natural product Anapehene B against MSSA and 4-fold more potent against MRSA, replacing one of the carbon atoms in the six-carbon ring of Analog **4** with a nitrogen atom (resulting in a pyridine) reduces its potency to that of Anaephene B (Figure 5, Analog **18**). Although the potency of Analog **18** is slightly reduced, it is likely more hydrophilic than Anaephene B (due to the pyridine ring) and the potentially useful in medicine (discussed below).

Additional biological assessment of Aanaephene B (2) and Analogs 4 and 18

Prompted by the antimicrobial activities, Analogs **4**, **18**, and Anaephene B (**2**) were selected for further evaluation of toxicity towards clinically relevant bacteria. To see of the analogs were effective against other gram-positive bacteria or just *S. aureus* we tested for antimicrobial activity against other clinically relevant gram-positive bacteria, such as *S. epidermis* and *E. faecalis.* The analogs were effective against *S. epidermis* and *E. faecalis* with MIC values comparable to those displayed against *S. aureus* (2-8 μg/mL) reported in detail in Kukla et al. 2021. We additionally tested the analogs against the gram-negative bacteria *A.*

baumannii (ATCC 19606) and *P. aeruginosa* (ATCC 27853). Neither of the analogs displayed antimicrobial activity against these two gram-negative pathogens. This is potentially indicative of the compounds having mechanism of action that is specific to gram-negative bacteria.

For use as antimicrobials in medicine, the analogs should not be toxic to mammalian cells. To probe cytotoxicity, a red blood cell hemolysis assay was performed. The blood cell hemolysis assay revealed that Analog **18** displayed significantly lower hemolytic activity (<1% at 100 μM) than Anaephene B (**2**) (80% at 100 μM) and Analog **4** (89% at 100 μM). Analog **18** was particularly interesting because it is both highly toxic to *Staphylococcus* and was well tolerated by mammalian red blood cells.

Finally, Anaephene B and two analogs (**4** and **18)** were evaluated in an MBC assay against MSSA. The MBC values for Anaephene B, Analog **4**, and Analog **18** were 16, 8, and 16 μg/ml, respectively (1). These MBC values are indicative of a bactericidal mechanism of action (MBC ≤4× MIC) (9).

Discussion

The results in this study suggest that an optimal analog structure consists of a 6–10 carbon long alkyl chain with an internal alkyne and no additional unsaturation. Analogs **4**, **8**, **11** and **18** all displayed high antimicrobial activity and interestingly an addition of a nitrogen to the head group resulted in hemolytic activity lower than 1% (Figure. 5). Therefore, Analog **4** appears to be the most promising compound for use in medicine due to its high potency and low levels of mammalian cytotoxicity. Our reasoning for developing the pyridine analogue is that the nitrogen is expected to make the molecule more water soluble. This is important because compounds with long alkyl chains are often highly hydrophobic. Hydrophobicity/lipophilicity is an important chemical property to consider in drug discovery due to its impact on drug

absorption, uptake, and metabolism (10). Hydrophobicity also plays a dominant role in promoting off-target binding as increased hydrophobicity leads to a higher likelihood of binding to unwanted cellular targets along with an increased risk of off-target based toxicity (10). For future directions, we can generate more pyridine analogues and assess biological activities.

In medicinal chemistry, heterocycles are regarded as incredibly useful because of their ability to manipulate the lipophilicity, polarity, and hydrogen bonding capabilities of a molecule. This in turn may lead to improved pharmacological, pharmacokinetic, toxicological, and physicochemical properties of a drug candidate or lead molecules (11). Thus, we believe we can improve drug-like properties of the analogs by replacing the phenol with a heterocycle. However, the phenol may have some significance to the mechanism of action, as methylation of the hydroxyl abolished all activity at 128 μg/mL in analog **9** (Figure 3). To improve drug-like properties, and retain similar chemical properties, bioisosteres can be utilized. Bioisosteres are molecules that result from the change of one atom or group to another similarly reacting atom or group (12). The purpose of utilizing bioisosteres is to replace the parent moiety with something that is physiochemically similar but is more likely to attenuate toxicity (12). Thus, I predict that the pyridinol head group in **18** provides the phenolic chemical properties that are important to the molecules activity while improving drug like properties and thus decreasing cell lysis. Analog **18** warrants further investigation to assess and drug-like properties.

Currently the mechanism of action of the Anaephene analogs is unknown, although speculations can be made based on their chemical structures and relative activities. I believe that due to the high lipophilicity, the mechanism of action involves interaction with the cell membrane. The Anaephene analogs are phenolic antimicrobials. Phenolic antimicrobials are thought to act by accumulating around and disrupting the bacterial cell membrane. Parabens are

a class of FDA approved antibiotics, used as preservatives in cosmetic products, that contain a phenolic moiety like that of the Anaephene analogs. Parabens interfere with the bacterial membrane and/or inhibit RNA and DNA synthesis (13). Unlike the commonly reported alkylphenols and phenolic antimicrobials, the Anaephene analogs in this study include a long alkyne-containing alkyl chain which represents an interesting moiety, unique to antibiotic development. Due to the high lipophilicity and long alkyl chain of the molecules along with their aliphatic properties, I propose that they interact with the bacterial cell membrane but not necessarily permeate through it. I hypothesize that the mechanism of action likely involves disruption of the bacterial cell membrane, leading to the death of the bacterial cell. However further examination is required to shine light on the mechanism of action and determine the potential for clinical application of the Anaepehene antibiotics.

References

1. Kukla, D. L., Canchola, J., Rosenthal, J. D., & Mills, J. J. (2021). Design, synthesis, and structure–activity relationship studies of the anaephene antibiotics. Chemical Biology & Drug Design, 98(2), 295–304. https://doi.org/10.1111/cbdd.13903
2. Centers for Disease Control and Prevention (U.S.). (2019). Antibiotic resistance threats in the United States, 2019. Centers for Disease Control and Prevention (U.S.). https://doi.org/10.15620/cdc:82532
3. Jim O'Neill. (2016). Tackling drug-resistant infections globally: Final report and recommendations. https://apo.org.au/node/63983
4. World Health Organization The World is Running Out of Antibiotics, WHO Report Confirms. 2017. [(accessed on 22 May 2022)]. Available online: https://www.who.int/news/item/20-09-2017-the-world-is-running-out-of-antibiotics-who-report-confirms
5. Plackett, B. (2020). Why big pharma has abandoned antibiotics. Nature, 586(7830), S50–S52. https://doi.org/10.1038/d41586-020-02884-3
6. Porras, G., Chassagne, F., Lyles, J. T., Marquez, L., Dettweiler, M., Salam, A. M., Samarakoon, T., Shabih, S., Farrokhi, D. R., & Quave, C. L. (2021). Ethnobotany and the Role of Plant Natural Products in Antibiotic Drug Discovery. Chemical Reviews, 121(6), 3495–3560. https://doi.org/10.1021/acs.chemrev.0c00922
7. Brumley, D., Spencer, K. A., Gunasekera, S. P., Sauvage, T., Biggs, J., Paul, V. J., & Luesch, H. (2018). Isolation and Characterization of Anaephenes A–C, Alkylphenols from a Filamentous Cyanobacterium (Hormoscilla sp., Oscillatoriales). Journal of Natural Products, 81(12), 2716–2721. https://doi.org/10.1021/acs.jnatprod.8b00650

8. Lipinski, C. A., Lombardo, F., Dominy, B. W., & Feeney, P. J. (2001). Experimental and computational approaches to estimate solubility and permeability in drug discovery and development settings 1PII of original article: S0169-409X(96)00423-1. The article was originally published in Advanced Drug Delivery Reviews 23 (1997) 3–25. 1. Advanced Drug Delivery Reviews, 46(1–3), 3–26. https://doi.org/10.1016/S0169-409X(00)00129-0
9. French, G. L. (2006). Bactericidal agents in the treatment of MRSA infections—The potential role of daptomycin. Journal of Antimicrobial Chemotherapy, 58(6), 1107–1117. https://doi.org/10.1093/jac/dkl393
10. McQueen, C. A., & Reilly, C. (Eds.). (2018). Respiratory toxicology (Third edition). Elsevier.
11. Martins, P., Jesus, J., Santos, S., Raposo, L., Roma-Rodrigues, C., Baptista, P., & Fernandes, A. (2015). Heterocyclic Anticancer Compounds: Recent Advances and the Paradigm Shift towards the Use of Nanomedicine's Tool Box. Molecules, 20(9), 16852–16891. https://doi.org/10.3390/molecules200916852
12. Holenz, J. (Ed.). (2016). Lead generation: Methods, strategies, and case studies. Wiley-VCH Verlag GmbH & Co. KGaA.
13. Halla, N., Fernandes, I., Heleno, S., Costa, P., Boucherit-Otmani, Z., Boucherit, K., Rodrigues, A., Ferreira, I., & Barreiro, M. (2018). Cosmetics Preservation: A Review on Present Strategies. Molecules, 23(7), 1571. https://doi.org/10.3390/molecules23071571

Figures

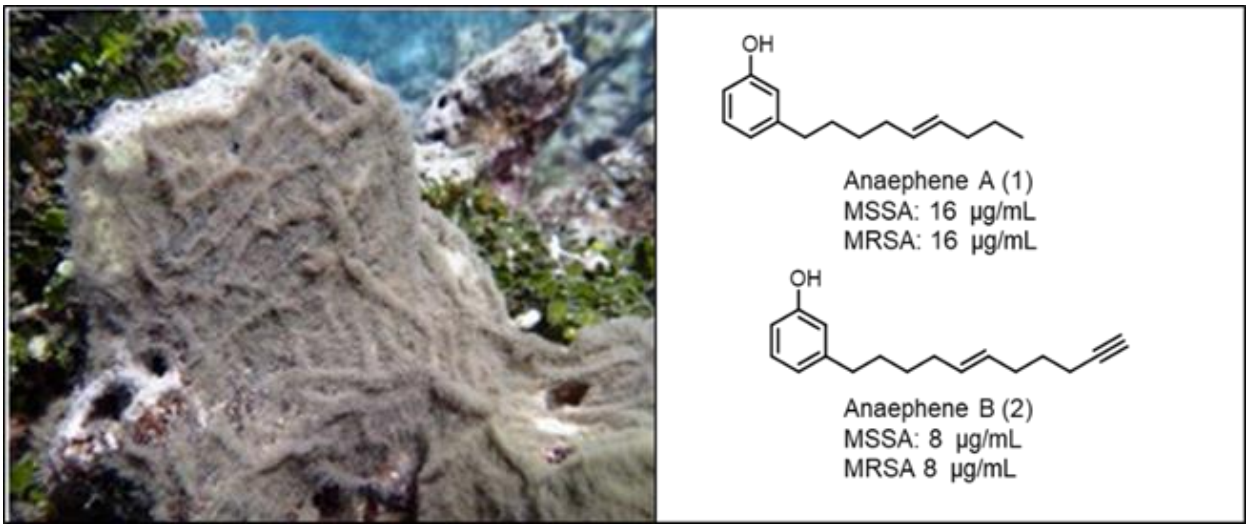

Figure 1: The Anaephene Natural products

(Right) Anaephenes A and B and their biological activities against methicillin resistant Staphylococcus aureus (MRSA) and Methicillin susceptible Staphylococcus aureus (MSSA) isolated from a filamentous cyanobacterium (VPG 16-59) from the genus *Hormoscilla* collected off the coast of Guam (Left) (Brumley D. 2018)

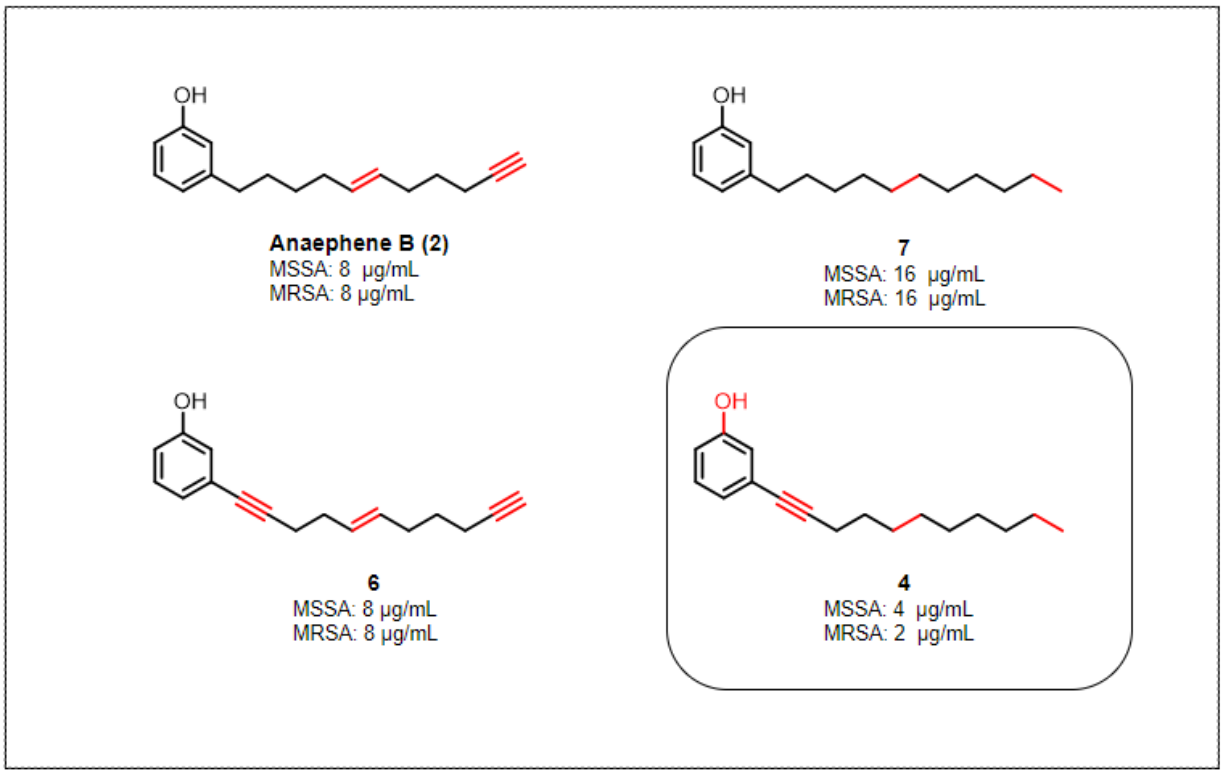

Figure 2: **Analogs from SAR study on Degrees of saturation**

Anaephene B (**2**) (top left) with analogs from SAR study on degree of saturation and MIC values, the most potent analog (**4**) is indicated in the box. Changes in unsaturation indicated in red.

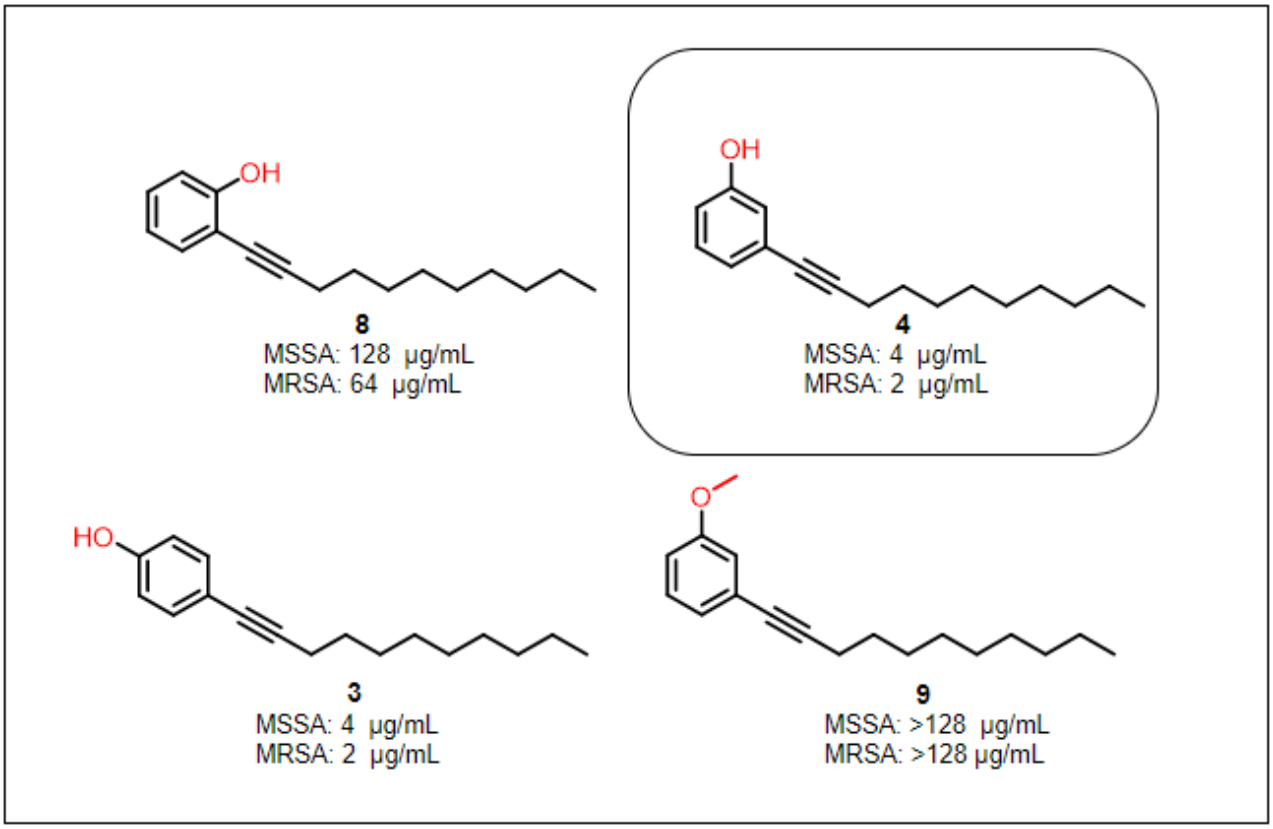

Figure 3: **Analogs from SAR study on hydroxy position**

Analogs from SAR stud on hydroxy position with MIC values Shown. Analogs with para (**3**), meta (**4**), ortho (**8**) orientation and methylated hydroxyl (**9**). Most potent analogue (**4**) indicated in box.

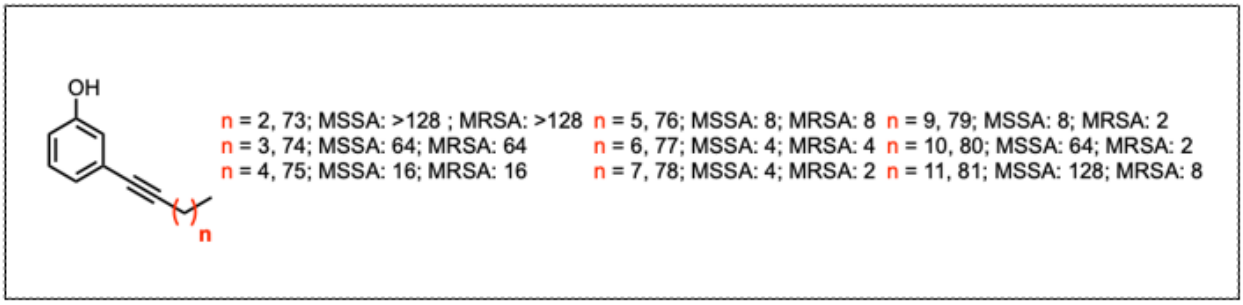

Figure 4: **Analogs from SAR study on chain length**

Analogs with carbon chain lengths varying from 3-11 after the internal alkyne. Carbons shown with resulting MIC values.

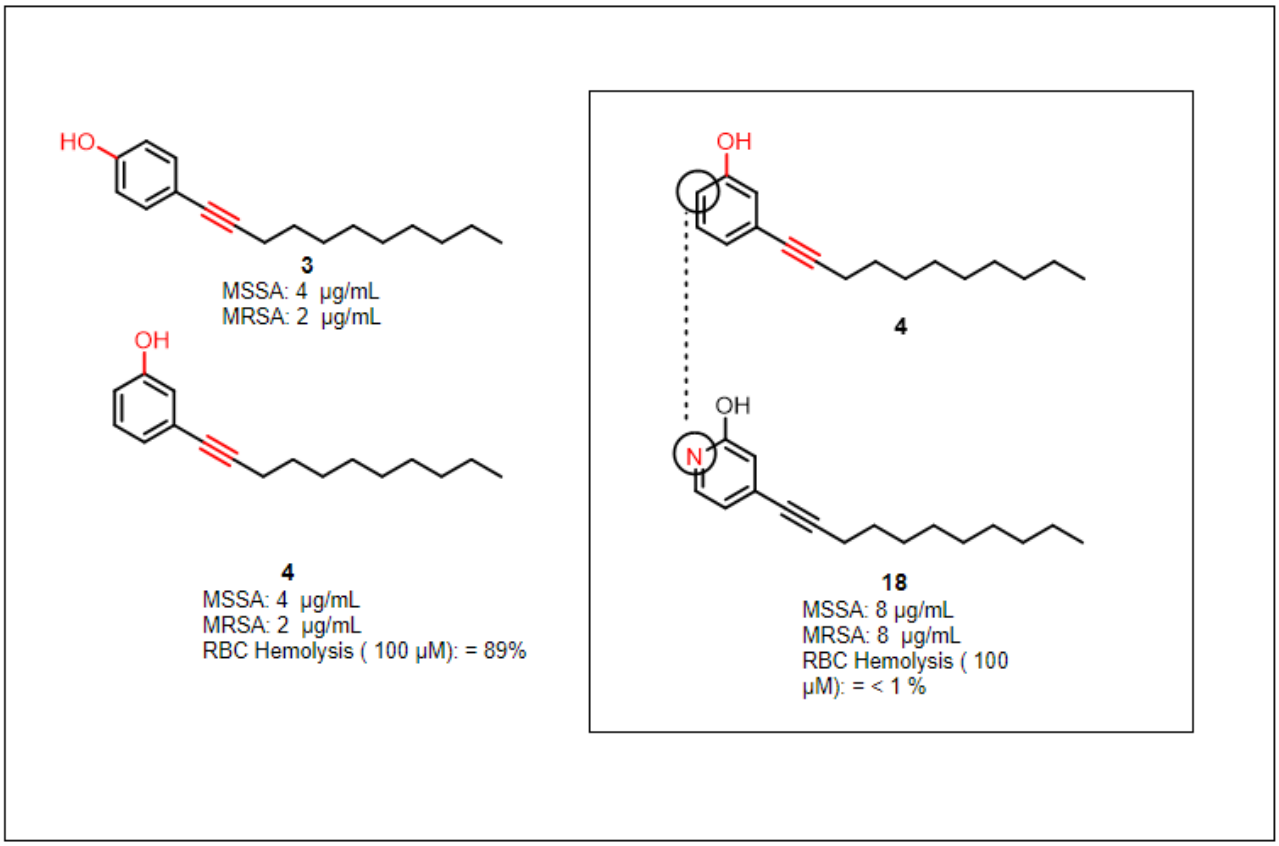

Figure 5: **Analog 18 contains a pyridine**

Most potent analogs that resulted from SAR study (left). Simplified nitrogen containing analogue **18** and resulting biological activity (right).

CHAPTER II: SYNTHESIS AND ANTIMICROBIAL ASSESMENT OF ALKYL PYRIDINOLS

Summary

The rapid syntheses of five novel alkyl pyridinols is reported along with antibacterial activity of the compounds against *Staphylococcus aureus* and mammalian cells. A Sonogashira cross-coupling reaction served as the key synthetic step to furnish the antibacterial pyridinol products. In this study, Analog JC-01-072 was created and found to possess an MIC value of 8 µg/ml towards *S. aureus*. Three analogs were selected for mechanism of action studies based on presumed safety towards mammalian cells. Analog JC-01-074 was found to possess bacteriostatic activity. Additionally, via propidium iodide staining and fluorescence microscopy, we showed that JC-01-074 disrupts the bacterial membrane and induces membrane deformities, indicating a membrane associated mechanism of action.

The work reported below is being prepared as J. Canchola, G, Donkor, A. Fasawe, P. Tawiah, E. Ayim, M. Engelke and J. Dahl "Alkyl Pyridinol compounds exhibit antimicrobial effects against Gram-positive bacteria".

Introduction

Due to misuse and overreliance on antibiotics, pathogenic bacteria are becoming resistant to many commonly used antibiotics (1). Consequentially, we are approaching an era where people die from bacterial infections that were once treatable. Considering their vast chemo diversity and variety of unique mechanisms of action available, natural products are an excellent avenue for antibiotic discovery (2). In previous work, we reported synthesis and structure activity studies of Anaephenes A and B and eighteen analogs (3,4). Within the series of analogs previously made, there was a particularly interesting group of alkylphenol analogs that exhibited

potent antimicrobial activities. One analog was a pyridine analog (**18**) that displayed potent activity against MRSA (8 μg/ml) and was not cytotoxic in a red blood cell hemolysis assay (3). The results of these preliminary evaluations and the implied desirable biological activity of the analogs, particularly analog (**18**), warranted further investigation.

Through additional SAR studies and lead optimization, new analogs with improved antimicrobial activities and drug-like properties can be generated. Using synthetic methods based on our reported synthesis of the anaephene natural products and analogs (3,4) we generated five analogs and tested for activity against multi-drug resistant community acquired USA 300 LAC *S. aureus* and toxicity against 3T3 mice cells. The strategy for designing the analogs was to investigate the significance of nitrogen position by generating analogs with nitrogen oriented meta (JC-01-072), ortho (JC-01-074) and para (EA-02-011) to the alcohol (Figure 6). We additionally generated analogs exploring the effects of adding an additional alkyl chain (JC-01-083) and a large electronegative halogen such as bromine (EA-02-009). The general synthetic procedure relied heavily on a Sonagashira cross-coupling reaction we previously reported on (3,4). However, utilizing a pyridine head group instead of alkyl phenol to generate the alkyl pyridine group of analogs (Figure 7). The reasoning for changing the phenolic head group to a pyridine is that it would increase water solubility and improve hydrogen bonding capabilities, which are important drug properties. Additionally, due to their ability to act as bioisosteres of amines, amides and nitrogen containing heterocycles, utilization of pyridines instead of other cyclic moieties is important in drug discovery (5).

The goal in this study was to design, synthesize and biologically assess a new group of anaephene analogs with improved drug-like properties for continuation of lead-optimization and potential preparation for preclinical examinations. Prior to this study, the mechanism of action of

the anaephene analogs was completely unknown. Due to the high lipophilicity and long alkyl chain of the anaephene analogs along with their aliphatic properties, we speculate the mechanism of action involves integration into the bacterial membrane, disrupting the cell wall, leading to death of the bacterial cell. We selected three of our five analogs for further testing to attempt to demystify the mechanism of action. We additionally tested synergy with clinically relevant antibiotics and anti-biofilm activity in biofilm inhibition and eradication assays.

Materials and Methods

Mammalian cell culture and MTT assay

3T3 cells (male mouse embryonic fibroblast Flp-In cells, Thermo Fisher) were cultured in D-MEM (Corning) with 10% Fetal Clone III (Cytiva Hyclone) and L-Glutamine (Alfa Aesar) at 37°C and 5% CO2. To determine compound toxicity, 3T3 cells were seeded at a density of 10,000 cells/well into 96-well plates (Fisherbrand) and cultured as described above. 16 hours later, culture medium was extracted and replaced by supplemented D-MEM without phenol red (Corning) containing individual compounds in the indicated concentrations. 1% SDS and 2% DMSO, equivalent to the volume of the DMSO in the highest compound concentration, were used as cell death and vehicle control, respectively. 16 hours after compound treatment culture medium was extracted again and replaced by fresh supplemented D-MEM without phenol red. Subsequently, 10 µl of 5mg/ml MTT reagent (Alfa Aesar) dissolved in DMSO was added to each well and cells were incubated for 2 hours at 37°C and 5% CO2. Next 85 µl of culture supernatant was removed from each well, mixed with 50 µl DMSO and incubated in an optical grade 96-well plate (Fisherbrand) in a shaking incubator at 37°C and 250 rpm. Absorbance of the MTT treated cell culture supernatant was measured at 540 nm in a ELx808 plate reader (Biotek).

MIC and MBC determination for USA300LAC

The minimal inhibitory and bactericidal concentrations of JC-01-072, JC-01-074 and EA-01-0019 against *S. aureus* USA 300 LAC were determined by following the CLSI guidelines for the broth microdilution antibiotic sensitivity testing protocol. Single colonies of USA 300 were inoculated into 5ml LB broth and incubated under shaking conditions for 20 hours. Overnight cultures were diluted to a final inoculum concentration of 5×10^5 CFU/ml (O.D.600 nm = 0.00001) in Mueller Hinton Broth (MHB) and dispensed into a 96-well polystyrene plate. Alkyl pyridine compounds were diluted into inoculated MHB to obtain desired concentrations, while ensuring DMSO concentrations remained below 5%. Following MIC determination, minimum bactericidal concentration (MBC) was determined by inoculating 10µl of culture on prewarmed LB agar plates from wells at 37°C to observe colony growth. The concentration at which no visible growth was observed after 20 hours was recorded as the MBC.

Growth curve Assay

Overnight USA 300 LAC cultures were diluted to an OD_{600} of 0.001 in tryptic soy broth (TSB) and incubated at 37 °C under shaking conditions (300 rpm) until OD_{600} of 0.2-0.3 (early log-phase). Cultures were transferred to a 96 well polystyrene plate, following which DMSO (control) or alkyl pyridine compounds were diluted into cultures to desired concentrations. Plates were then incubated under aforementioned conditions and optical densities were measured at 10-minute intervals in a Tecan Spark microplate reader for 16-18 hours.

Propidium Iodide Fluorescence Assay

USA 300 LAC grown to early log phase and treated with DMSO (control), an alkyl pyridine, vancomycin or SDS at desired concentrations and grown at 37°C (300rpm). After a 1-hour treatment, cells were collected, washed twice, and resuspend in PBS (pH =7.4). Cells were

subsequently stained with 1μM propidium iodide and fluorescence intensity was measured at excitation and emission wavelengths of 535 nm and 615 nm respectively.

Fluorescence Microscopy

Overnight USA 300 cultures were diluted in TSB to OD_{600} of 0.01 and incubated under shaking conditions at 37 °C until mid-log phase (OD_{600} of 0.2-0.3). Cultures were either left untreated or treated with DMSO, daptomycin (positive control) or with JC-01-074. Cells were collected at 15 and 60 minutes, washed and resuspended in fresh TSB. Cells were subsequently stained with 5μg/ml DAPI or Nile Red for 10 minutes, washed and resuspended in fresh TSB. Cells were then imaged on 1% agarose gel pads and via fluorescence microscopy using a Leica SP8 confocal microscope. A 63 ×/1.40 oil objective was used, with a white light laser set to a wavelength of 488 nm. Fluorescence was detected between the wavelengths of 500–560 nm, with 8×line averaging.

Biofilm Inhibition and Eradication Assay

Overnight USA 300 LAC cultures were diluted approximately 1000-fold in TSB and incubated under shaking conditions at 37°C until mid-log phase. Cultures were subsequently diluted to approximately 4×10^6 CFU/ml and dispensed into a polystyrene 96 well plate containing DMSO (control), vancomycin, or alkyl pyridine compounds. Periphery wells were filled with PBS to limit evaporation and plates were incubated without agitation at 37°C for 24 hours. Following incubation, planktonic cells were removed, and wells were washed with PBS. Biofilm formation was evaluated via crystal violet staining measured 595nm in a Tecan 200 infinite pro microplate reader. To evaluate biofilm eradication, planktonic cells were removed from preformed USA 300 LAC biofilms grown (as described aforehand) under static conditions for 24 hours. Wells containing biofilms were washed with PBS and filled with TSB containing

DMSO (control), vancomycin, or alkyl pyridine compounds. Plates were subsequently incubated under static conditions for 24 hours, after which reduction in biofilms was evaluated via crystal violet staining measured 595nm in a Tecan 200 infinite pro microplate reader.

Evaluation of antibiotic synergy with JC-01-074

The checkerboard assay was employed to determine if JC-01-074 had synergistic effects in combination with conventional antibiotics. Antibiotics tested in combination were initially serially diluted two-fold in MHB on a longitudinal axis in a polystyrene 96 well plate. JC-01-074 was then serially diluted two-fold across the 96 well plate horizontal axis. Plates were inoculated with USA 300 LAC cultures to a final inoculum concentration of 5 $x10^5$ CFU/ml OD_{600} of 0.0001. Plates were incubated overnight at 37°C for 20 hours after which growth was measured at 600nm in a Tecan 200 infinite pro microplate reader. The scheme for antimicrobial dilutions for the checkerboard assay was adapted from established methods (1). The fractional inhibitory concentration was calculated as the ratio of the MIC of the antimicrobial when used alone over the MIC of the antibiotic in combination. Classification of interactions was based on the FIC index, calculated as the sum of the FICs of the two antimicrobials was calculated as the sum of the FICs of the two antimicrobials tested in combination. Interactions were categorized as synergistic (≤0.5), additive/no interaction (≤0.5 to ≤2), and antagonistic (>2).

General experimental procedures for synthesis and characterization of the analogs

1H and 13C NMR spectra were obtained on a Bruker 400 MHz Avance III spectrometer or Bruker 500 MHz Avance III spectrometer in $CDCl_3$ unless otherwise noted. Chemical shifts are reported with the residual solvent peak used as an internal standard ($CDCl_3$ = 7.26 ppm for 1H and 77.16 ppm for 13C). High-resolution mass spectra were obtained using positive mode electrospray ionization (ESI+) on a Thermo Scientific Q Exactive hybrid Quadripole-Orbitrap

mass spectrometer. Reactions were monitored by TLC analysis (silica gel 60 F254, 250 mm layer thickness) and visualized with a 254 nm UV light. Flash column chromatography was performed with silica gel 60 (230-400 mesh). All starting materials and solvents were purchased from a commercial chemical company and used as received.

5-(undec-1-yn-1-yl) pyridin-3-ol (JC-01-072)

To a solution of 5-iodopyridine-3-ol (100 mg, 0.45 mmol) in acetonitrile (2.15 mL) was added 1-undecyne (0.27 mL, 1.36 mmol), solid CuI (17.2 mg, 0.09 mmol) and $PdCl_2(PPh_3)_2$ (15.9 mg, 0.023 mmol). Then, Et_3N (0.21 mL, 1.50 mmol) was added dropwise, and the reaction was left to stir at room temperature for 1 hr and at 60 °C for 3 hrs. A mixture of product and Triethylamine salt resulted and was quenched with saturated $NaHCO_3$ (10 mL), the aqueous layer was extracted with Ethyl acetate (3 × 10 mL). The combined organic layers were washed with brine, dried (MgSO4), filtered, and concentrated under reduced pressure. The residue was purified by flash column chromatography (0-100% Ethyl acetate /Hexanes) to afford **JC-01-072** as a brown-yellow solid (53.0 mg, 47 % yield): 1H NMR ($CDCl_3$, 400 MHz) δH 8.11 (s, 2H), 7.28 (s, 1H), 2.40 (t, J = 7.1 Hz, 2H), 1.60 (p, J = 6.9 Hz, 2H), 1.43 (p, J = 6.8 Hz, 2H), 1.34-1.28 (m, 10H); 0.88 (t, J = 6.7 Hz, 3H); 13C NMR ($CDCl_3$, 100 MHz) δC 154.4, 142.4, 135.2, 127.3, 123.0, 94.9, 77.4, 32.0, 30.0, 29.4, 29.3, 29.1, 28.7, 22.8, 19.6, 14.2; HRESIMS m/z 246.1857 [M+H]+ (calculated for $C_{16}H_{23}NO$, 246.1858).

6-(undec-1-yn-1-yl) pyridin-2-ol (JC-01-074)

To a solution of 6-iodopyridine-2-one, (100 mg, 0.45 mmol) in acetonitrile (2.15 mL) was added 1-undecyne (0.27 mL, 1.36 mmol), solid CuI (17.2 mg, 0.09 mmol) and $PdCl_2(PPh_3)2$ (15.9 mg, 0.023 mmol). Then mL Et_3N (0.21 mL, 1.50 mmol) was added dropwise, and the reaction was left to stir at room temperature for 1 hr and at 60 °C for 3 hrs. A

mixture of product and Triethylamine salt resulted and was quenched with saturated $NaHCO_3$ (10 mL), the aqueous layer was extracted with Ethyl acetate (3 × 10 mL). The combined organic layers were washed with brine, dried ($MgSO_4$), filtered, and concentrated under reduced pressure. The residue was purified by flash column chromatography (0-100% Ethyl acetate /Hexanes) to afford **JC-01-074** as a yellow solid (10.2 mg, 9.2% yield) :1H NMR ($CDCl_3$, 400 MHz) δH 7.29 (d, J = 6.5 Hz, 1H), 6.58 (s, 1H), 6.24 (d, J = 6.4 Hz, 1H), 2.41 (t, J = 7.1 Hz, 2H), 1.60 (p, J = 7 Hz, 2H), 1.42 (p, J = 6.8 Hz, 2H), 1.34-1.25 (m, 10H), 0.86 (t, J = 6.6 Hz, 3H); 13C NMR (CDCl3, 100 MHz) δC 164.9, 138.4, 134.2, 122.5, 110.3, 98.3, 78.4, 32.0, 30.0, 29.4, 29.2, 29.1, 28.4, 22.8, 19.7, 14.2; HRESIMS m/z 246.1854 [M+H]+ (calculated for C16H23NO, 246.1858).

2-bromo-6-(undec-1-yn-1-yl) pyridin-4-ol (EA-02-009)

To a solution of 2,6-dibromopyridine-ol (75.0 mg, 0.29 mmol) in acetonitrile (2.15 mL) was added 1-undecyne (0.16 mL, 0.89 mmol, solid CuI (11.3 mg, 0.059 mmol) and $PdCl_2(PPh_3)_2$ (10.4 mg, 0.015 mmol). Then Et3N (0.14 mL, 0.98 mmol) was added dropwise, and the reaction was left to stir at room temperature for 1 hr and at 60 °C for 3 hrs. A mixture of product and Triethylamine salt resulted and was quenched with $NaHCO_3$ (10 mL), the aqueous layer was extracted with Ethyl acetate (3 × 10 mL). The combined organic layers were washed with brine, dried (MgSO4), filtered, and concentrated under reduced pressure. The residue was purified by flash column chromatography (0-100% Ethyl acetate /Hexanes) to afford **EA-02-009** as a brown oil (24.1 mg, 32 % yield): 1H NMR ($CDCl_3$, 400 MHz) δH 7.01 (d, J = 1.5 Hz, 1H), 6.90 (d, J = 1.6 Hz, 1H), 2.34 (t, J = 7.1 Hz, 2H), 1.52 (p, J = 7.0 Hz, 2H), 1.37-1.26 (m, 12 H), 0.88 (t, J = 6.2 Hz, 3H); 13C NMR ($CDCl_3$, 125 MHz) δC 175.1, 139.7, 133.2, 115.7, 115.3, 95.0, 77.5, 31.9, 29.4, 29.3, 29.1, 28.9, 28.1, 22.7, 19.3, 14.1; HRESIMS m/z 324.0958 [M+H]+

(calcd for $C_{16}H_{22}BrNO$, 324.0963).

2,6-di(undec-1-yn-1-yl) pyridin-4-ol (JC-01-083)

To a solution of 2,6-dibromopyridine-ol (75.0 mg, 0.29 mmol) in acetonitrile (2.15 mL) was added 1-undecyne (0.16 mL, 0.89 mmol, solid CuI (11.3 mg, 0.059 mmol) and $PdCl_2(PPh_3)_2$ (10.4 mg, 0.015 mmol). Then Et3N (0.14 mL, 0.98 mmol) was added dropwise, and the reaction was left to stir at room temperature for 1 hr and at 60 °C for 3 hrs. A mixture of product and Triethylamine salt resulted and was quenched with NaHCO3 (10 mL), the aqueous layer was extracted with Ethyl acetate (3 × 10 mL). The combined organic layers were washed with brine, dried ($MgSO_4$), filtered, and concentrated under reduced pressure. The residue was purified by flash column chromatography (0-100% Ethyl acetate/Hexanes) to afford **JC-01-083** as a brown-yellow oil (16.0 mg, 21 % yield): 1H NMR ($CDCl_3$, 400 MHz) δH 6.67 (s, 2H), 2.35 (t, J = 7.1 Hz, 4H), 1.54 (p, J = 7.1 Hz, 4H), 1.39-1.26 (m, 24H), 0.88 (t, J = 6.6 Hz, 6H); 13C NMR ($CDCl_3$, 100 MHz) δC 161.1, 137.0, 118.4, 96.7, 77.4, 32.0, 30.0, 29.4, 29.3, 29.1, 28.2, 22.8, 19.5, 14.2; HRESIMS m/z 396.3264 [M+H]+ (calculated for $C_{27}H_{41}NO$, 396.3266).

2-(undec-1-yn-1-yl) pyridin-4-ol (EA-02-011)

To a solution of 2-bromo-6-(undec-1-yn-1-yl) pyridin-4-ol (**EA-02-009**) (42.8 mg, 0.13 mmol) in dry THF (0.70 mL) at –78 °C, was added n-BuLi (0.12 mL, 1.32 mmol) dropwise. The reaction was left to stir for 20 minutes, then quenched with saturated NH_4Cl (10mL) and extracted with Ethyl ether (3 × 10 mL). The combined organic layers were washed with brine, dried ($MgSO_4$) and concentrated. Reaction was purified under silica gel column chromatography using (0-10 % Methanol/Dichloromethane) to afford **EA-02-011** as a brown oil (12.4 mg, 38% yield): 1H NMR ($CDCl_3$, 400 MHz) δH 7.67 (d, J = 6.9 Hz. 1H),

6.65 (d, J = 2.2 Hz, 1H), 6.51 (dd, J = 6.9, 2.3 Hz, 1H), 2.33 (t, J = 7.1 Hz, 2H), 1.52 (p, J = 7.0 Hz, 2H), 1.37-1.24 (m, 12H), 0.86 (t, J = 6.6 Hz, 3H); 13C NMR (CDCl3, 100 MHz) δC 177.4, 140.6, 135.7, 119.9, 115.8, 96.3, 75.2, 32.0, 29.6, 29.4, 29.3, 29.1, 28.2, 22.8, 19.5, 14.2; HRESIMS m/z 246.1853 [M+H]+ (calcd for $C_{16}H_{23}NO$, 246.1858).

Results

Chemical Synthesis

Based off findings from previous analogs and SAR studies (3) we proposed a group of five new Anaephene analogs comprising of five long alkyl chain pridinols aiming to explore the significance of the nonpolar, lipophilic structure and increase drug-like properties. The group of proposed analogs were synthesized based on a modular synthetic pathway we had previously established and utilized to synthesize a family of Anaephene analogs with varying antimicrobial properties (3). We synthesized the analogs in this study via a Sonagashira cross-coupling reaction, which allowed us to attach a cyclic head group to an alkyne-containing alkyl chain (Figure 7). The reaction relies on the reactivity of a terminal alkyne with an aryl or vinyl halide. Which, with help from a catalyst, reacts to form a carbon-carbon bond. By utilizing different head groups containing halides, bromine, or iodide, we were able to obtain JC-01-72, JC-01-74, JC-01-083 and EA-02-009 as clear-yellow oils. Leftover EA-02-009 was taken and set up for hydrogenation with n-BuLi to remove the attached bromine and yield us EA-02-011 as a brown oil. (Figure 7).

Compounds were slightly toxic

To gauge the potential for toxicity of our analogs, we tested for cytotoxicity in a MTT assay with 3T3 mouse embryonic fibroblast cells. Cells were treated with different concentrations of the alkyl pyridine compounds for 24 hours and absorbance of the MTT treated

cell culture supernatant was measured at 540 nm (Tables 1 & 2). Absorbances were plotted against concentrations of compound added to elude IC50, the concentration of a drug required for 50% metabolic inhibition, for each compound (Figure S2). We found that JC-01-072 had the highest IC50 (37.6 µg/ml) indicating the concertation at which a drug is toxic against eukaryotic 3T3 cells. Compounds EA-02-009 (34.6 µg/ml) and JC-01-083 (30.9 µg/ml) displayed similar IC50 concentrations. Conversely JC-01-074 lagged with a lower IC50 (25.2 µg/ml) and EA-02-11 displayed the lowest IC50 (10.7 µg/ml) indicating cytotoxicity at low concentrations.

JC-01-074 is Bactericidal

Considering the potency of the alkyl pyridine analogs at limiting gram-positive growth, we explored their activities against the multi-drug resistant community acquired USA 300 LAC *S. aureus* strain. Using CLSI broth microdilution guidelines (6), the MIC values for JC-01-72, JC-01-74 and EA-02-009 were determined. Following MIC determination, mean bactericidal concentration (MBC) were identified for the aforementioned alkyl pyridines (Table 3). We found that while JC-01-72 completely suppressed growth in USA 300 LAC at a 2-fold lower MIC (8µg/ml) compared to JC-01-074 (16µg/ml), its MBC was significantly higher (>128µg/ml) compared to JC-01-074(16µg/ml), indicating bacteriostatic activity at concentrations tested (Table 3). Surprisingly, EA-02-009, which had a relatively higher MIC of 32µg/ml, had an MBC >128µg/ml.

JC-01-074 inhibits growth during log phase

Considering their divergent antimicrobial effects, we proceeded to assess the impact of JC-01-072 and JC-01-074 on the growth of actively dividing logarithmic phase USA 300 LAC. We found that 0.5X MIC of JC-01-074 delayed growth until stationary phase by approximately 6-8 hours while treatment at its MIC led to total growth arrest of logarithmic phase cultures for

16-18 hours. On the other hand, JC-01-072 had little to no growth inhibitory effects on logarithmic phase USA 300 LAC (Figure 8).

JC-01-074 disrupts bacterial membrane

The high calculated logP values of alkyl pyridine in this study indicates high lipophilicity and a potential for these compounds to incorporate into and disrupt lipid membranes (7). We therefore determined if JC-01-072, JC-01-074 and EA-02-0019 antibacterial activity involved membrane damage using a propidium iodide (PI) uptake assay. In the event that the inner membrane is compromised, PI, which is considerably cell impermeable, can traverse the membrane, intercalate with DNA and exhibit enhanced fluorescence (8). We found that 1 hour treatment with MIC of JC-01-074 (16µg/ml) resulted in about five-fold higher PI fluorescence compared to the DMSO treated control or 1X MIC of JC-01-072 (Figure 9). The extent of membrane damage was found to increase as the dose of JC-01-074 increased (Figure 10). Conversely, JC-01-072 and EA-02-009 exerted minimal changes in PI intensity even at 2X MIC after 60 minutes of exposure (Figure 9).

JC-01-074 limits biofilm formation

S. aureus is notorious for its ability to form biofilms on a variety of surfaces, which presents a unique treatment challenge (9). However, studies on membrane targeting antimicrobials have revealed their potential for curtailing biofilm formation (9,10). We therefore explored the potential of JC-01-74 to inhibit biofilm formation or reduce established biofilms in comparison to vancomycin (Figure 11). Treatment with JC-01-074 significantly limited biofilm formation (approximately 60-70%) at MIC and 2X MIC as opposed to vancomycin, which failed to significantly inhibit biofilm formation even at 2X MIC and 4X MIC. Conversely, neither JC-01-074 nor vancomycin could successfully reduce established biofilms at

concentrations tested, ruling out potentially biofilm eradication properties.

No significant synergistic effects with clinically relevant antibiotics

Membrane disruption has been demonstrated to potentiate the activity of certain conventional antibiotics in both gram positive and negative bacteria (9,11). We hypothesized that JC-01-74 membrane disrupting effects could increase that activity of antibiotics by potentially increasing their intracellular influx. Six groups of antibiotics were tested in combination with JC-01-074 in a checkerboard assay according to established protocols (12). Antibiotic concentrations were prepared by microdilution in Mueller Hinton broth to obtain final concentrations as outlined in the 96 well plate scheme for each antibiotic tested (Fig S1). Overnight USA 300 LAC cultures were diluted to a final CFU/ml of 5X105 Mueller Hinton in 96 well plates together with antibiotics tested. Plates were incubated at 37°C at 200 rpm for 20 hours after which OD600 values were measured. Fractional Inhibitory Concentrations (FIC) calculations were made using the lowest concentration of both antibiotics that completely inhibited growth. The sum of FIC values indicated that no antibiotic tested interacted synergistically with JC-01-74 (Figure 12). The combination of ampicillin and gentamicin had additive effects in combination with JC 01-074 while other antibiotics tested had no interaction in combination with JC-01-074

Discussion

As a continuation of our previous synthetic efforts to improve the drug like properties of the Anaephene natural product analogs, we designed the five analogs in this study. Which were designed based off the lead analogs **4** and **18** from previous studies (3). Our rationale for the new round of analogs was that the incorporation of nitrogen into the cyclic headgroup could make the molecules more drug-like and reduce cytotoxic potential. This previously supported in analog **18**

which demonstrated retained biological activity and reduced hemolytic activity (3). We believe that the pyridinol head group in the new analogs makes the molecules more polar and water soluble. This is important because due to the long alkyl chain, our molecules are relatively lipophilic. Lipophilicity is an important property to consider in drug discovery because it has an impact on drug absorption, uptake, and metabolism. Lipophilicity also plays a dominant role in promoting off-target binding as increased lipophilicity leads to a having a higher likelihood of binding to unwanted cellular targets. Thus, potentially increases the risk of toxicity (13). Therefore, introducing heteroatoms into the ring, making the molecule more polar and therefore more hydrophilic, may help in reducing the risk of toxicity and improve the drug-like properties. Additionally, heterocyclic compounds are thought to be more versatile in drug development due to their ability to manipulate lipophilicity, polarity, and hydrogen bonding capabilities of a molecule. This in turn may lead to improved pharmacological, pharmacokinetic, toxicological, and physicochemical properties of a drug candidate or lead molecules (14).

Unfortunately, all of the compounds displayed cytotoxic activity against 3T3 mice fibroblasts. Typically, 0-50 µg/ml is considered toxic (15), therefore EA-02-011 was highly toxic (10.7 IC50 µg/ml) and the rest of the analogs were weakly toxic. Though not favorable, low levels of toxicity are not always detrimental to a molecules drug candidacy. What is more important is the therapeutic index (TI), which is a ratio comparing range concentrations of a drug that has a therapeutic effect with concertation that causes toxicity (16). In drug deployment, a TI of about 10 or a 10-fold difference between therapeutic concertation and toxic concertation, is typically desired. However, drugs with lower TI's can still considered safe and effective if their benefits outweigh the risks (16). Such would be the case, especially with life-threatening bacterial infections. As we are only preliminarily assessing the compounds, in vitro and in a non-

clinical setting, we cannot extrapolate therapeutic indices. However, by referencing the MTT and MIC assay data, we can make predictions and select potential lead candidates, being compounds that may be more likely to yield larger safety windows or acceptable TI's. Compounds JC-01-072, JC-01-074 and EA-02-09 displayed the highest IC50 concentrations, around 25-38 ug/ml, with JC-01-074 having the highest at 37.6 µg/ml. Though, EA-02-09 has a relatively high MIC (32 µg/ml) only about 2.6 µg/ml difference from IC50, the safety window would be far too low. With an MIC of 16 µg/ml, the safety window for JC-01-074 would also be very low, with a difference of only 9.2 µg/ml. Fortunately, the IC50 of JC-01-072 was nearly 5-fold the MIC. Based off potential for having a greater safety window, JC-0-072 is our lead candidate.

We do not have a concrete explanation for the difference in biological activities for the analogs. However, predictions can be made based off the molecular structures, with emphasis on nitrogen position. Initially we hypothesized that due to the aliphatic structure of the compounds, they would incorporate into the cell membrane and disrupt it. However, for all but one of our analogs this was not supported by the data as only JC-01-074 was shown to disrupt the bacterial membrane in a PI fluorescence assay and microscopy. Our analogs are relatively lipophilic and low molecular weight (200-350 g/mol). Membrane permeable drugs tend to be those that are small and highly lipophilic. (17). Thus, we predict that our analogs permeate the membrane and interrupt an intracellular metabolic process, yielding the displayed bacteriostatic activity. We can attempt to rationalize the variance in activities that resulted from the different nitrogen position for JC-01-072 and EA-02-011, with principles of aromatic resonance with electron withdrawing groups and electron donating groups. Pyridine resonance yields nucleophilic susceptibility and the electron donating groups such as secondary alcohols, direct electrophilic substitutions (18). Changing nitrogen position changes these directing properties and positions of susceptibility. We

expect these changes may lead to varying hydrogen binding and salt forming capabilities. Only JC-0-074 displayed bactericidal activity and was shown to disrupt bacterial cell membranes. We speculate this is the case because JC-01-074 contains a cyclic amide. Cyclic amides, or lactams, are commonly utilized in drug discovery because of their versatility and use in a variety of potential therapeutic applications, such as diabetes, cancer, and infectious diseases (19,20). The proximity of the nitrogen's electron lone pair could allow it to be drawn into the secondary alcohol, increasing basicity and nucleophilicity. This could additionally offer more hydrogen bonding capabilities. We believe that the amide functional group in JC-01-074 increases hydrogen bonding and salt formation. Based on our findings and speculations, we hypothesize, that the mechanism of action of JC-01-074 involves incorporation into the cell membrane along with formation of JC-01-074 salts or additional complexes. This could disrupt osmotic equilibrium, many other membrane potential based functions, or mechanically perturb the membrane.

Future directions for this study may involve further investigation into the mechanism of action. To test for JC-01-074 interacting or inserting into the bacterial membrane, we can utilize a fluorescent-probe tagged JC-01-074 to visualize its localization along the membrane. Another experiment we can use to explore the membrane permeation capabilities of our analogs is via a parallel artificial membrane permeability assay (PAMPA), which is widely used in the pharmaceutical industry as a high throughput permeability assay to assess membrane permeability and predict oral absorption (20). General next steps for our potential lead compounds, JC-01-072 and JC-01-74, would include further lead optimization through more SAR studies to increase the therapeutic windows directly followed by ADMET/PK studies to prepare for preclinical investigations and in vivo studies. The compounds produced in this study

did not eradicate biofilms and were not synergistic with tested clinically relevant antibiotics, however they could be useful leads for further development. The analogs displayed antimicrobial activities against USA 300 LAC methicillin resistant s. aureus with low levels of toxicity against 3T3 mice fibroblasts. Additionally, JC-10-074 was particularly interesting as it has a suggested mechanism of action involving membrane disruption and displayed bactericidal activity and inhibited biofilm formation. Considering the findings from this study along with the significance and relevance of pyridines in drug discovery, we believe the analogs we generated can serve as modular molecular templates for future efforts in drug development and discovery.

References

1. Wright, P. M., Seiple, I. B., & Myers, A. G. (2014). The Evolving Role of Chemical Synthesis in Antibacterial Drug Discovery. Angewandte Chemie International Edition, 53(34), 8840–8869. https://doi.org/10.1002/anie.201310843
2. Porras, G., Chassagne, F., Lyles, J. T., Marquez, L., Dettweiler, M., Salam, A. M., Samarakoon, T., Shabih, S., Farrokhi, D. R., & Quave, C. L. (2021). Ethnobotany and the Role of Plant Natural Products in Antibiotic Drug Discovery. Chemical Reviews, 121(6), 3495–3560. https://doi.org/10.1021/acs.chemrev.0c00922
3. Kukla, D. L., Canchola, J., Rosenthal, J. D., & Mills, J. J. (2021). Design, synthesis, and structure–activity relationship studies of the anaephene antibiotics. Chemical Biology & Drug Design, 98(2), 295–304. https://doi.org/10.1111/cbdd.13903
4. Kukla, D. L., Canchola, J., & Mills, J. J. (2020). Synthesis of the Cyanobacterial Antibiotics Anaephenes A and B. Journal of Natural Products, 83(6), 2036–2040. https://doi.org/10.1021/acs.jnatprod.0c00279
5. Hamada, Y. (2018). Role of Pyridines in Medicinal Chemistry and Design of BACE1 Inhibitors Possessing a Pyridine Scaffold. In P. P. Pandey (Ed.), Pyridine. InTech. https://doi.org/10.5772/intechopen.74719
6. Weinstein, M. P., & Patel, J. B. (2018). Methods for dilution antimicrobial susceptibility tests for bacteria that grow aerobically: M07-A11 (11. edition). Committee for Clinical Laboratory Standards.

7. Chandrasekaran, B., Abed, S. N., Al-Attraqchi, O., Kuche, K., & Tekade, R. K. (2018). Computer-Aided Prediction of Pharmacokinetic (ADMET) Properties. In Dosage Form Design Parameters (pp. 731–755). Elsevier. https://doi.org/10.1016/B978-0-12-814421-3.00021-X
8. Boulos, L., Prévost, M., Barbeau, B., Coallier, J., & Desjardins, R. (1999). LIVE/DEAD® BacLightTM: Application of a new rapid staining method for direct enumeration of viable and total bacteria in drinking water. Journal of Microbiological Methods, 37(1), 77–86. https://doi.org/10.1016/S0167-7012(99)00048-2
9. Otto, M. (2008). Staphylococcal Biofilms. In T. Romeo (Ed.), Bacterial Biofilms (Vol. 322, pp. 207–228). Springer Berlin Heidelberg. https://doi.org/10.1007/978-3-540-75418-3_10
10. MacNair, C. R., & Brown, E. D. (2020). Outer Membrane Disruption Overcomes Intrinsic, Acquired, and Spontaneous Antibiotic Resistance. mBio, 11(5), e01615-20. https://doi.org/10.1128/mBio.01615-20
11. Kaplan, C. W., Sim, J. H., Shah, K. R., Kolesnikova-Kaplan, A., Shi, W., & Eckert, R. (2011). Selective Membrane Disruption: Mode of Action of C16G2, a Specifically Targeted Antimicrobial Peptide. Antimicrobial Agents and Chemotherapy, 55(7), 3446–3452. https://doi.org/10.1128/AAC.00342-11
12. Bellio, P., Fagnani, L., Nazzicone, L., & Celenza, G. (2021). New and simplified method for drug combination studies by checkerboard assay. MethodsX, 8, 101543. https://doi.org/10.1016/j.mex.2021.101543
13. McQueen, C. A., & Reilly, C. (Eds.). (2018). Respiratory toxicology (Third edition). Elsevier.

14. Gomtsyan, A. (2012). Heterocycles in drugs and drug discovery. Chemistry of Heterocyclic Compounds, 48(1), 7–10. https://doi.org/10.1007/s10593-012-0960-z
15. Bich-Loan, N. T., Kien, K. T., Thanh, N. L., Kim-Thanh, N. T., Huy, N. Q., The-Hai, P., Muller, M., Nachtergael, A., Duez, P., & Thang, N. D. (2021). Toxicity and Anti-Proliferative Properties of Anisomeles indica Ethanol Extract on Cervical Cancer HeLa Cells and Zebrafish Embryos. Life, 11(3), 257. https://doi.org/10.3390/life11030257
16. Tamargo, J., Le Heuzey, J.-Y., & Mabo, P. (2015). Narrow therapeutic index drugs: A clinical pharmacological consideration to flecainide. European Journal of Clinical Pharmacology, 71(5), 549–567. https://doi.org/10.1007/s00228-015-1832-0
17. Bennion, B. J., Be, N. A., McNerney, M. W., Lao, V., Carlson, E. M., Valdez, C. A., Malfatti, M. A., Enright, H. A., Nguyen, T. H., Lightstone, F. C., & Carpenter, T. S. (2017). Predicting a Drug's Membrane Permeability: A Computational Model Validated With in Vitro Permeability Assay Data. The Journal of Physical Chemistry B, 121(20), 5228–5237. https://doi.org/10.1021/acs.jpcb.7b02914
18. MLP Reddy. (2018). JPhCPhB C Photochemistry Review. https://doi.org/10.13140/RG.2.2.33202.50885
19. Saldívar-González, F. I., Lenci, E., Trabocchi, A., & Medina-Franco, J. L. (2019). Exploring the chemical space and the bioactivity profile of lactams: A chemoinformatic study. RSC Advances, 9(46), 27105–27116. https://doi.org/10.1039/C9RA04841C
20. Di, L., Kerns, E. H., Fan, K., McConnell, O. J., & Carter, G. T. (2003). High throughput artificial membrane permeability assay for blood–brain barrier. European Journal of Medicinal Chemistry, 38(3), 223–232. https://doi.org/10.1016/S0223-5234(03)00012-6

Tables

Table 1. Minimal inhibitory concentration and minimal bactericidal concentrations of antimicrobials tested against USA 300 LAC.

	USA 300 LAC	
Antimicrobial	MIC(µg/ml)	MBC (µg/ml)
EA-02-009	32	>128
JC-01-072	8	>128
JC-01-074	16	16
Vancomycin	1	-
Ampicillin	2.33	-
Chloramphenicol	4	-
Gentamicin	1	-
Ciprofloxacin	16	-
Doxycycline	0.125	-

Table 2. Viability of 3T3 cells treated with tested compounds for 24 hours, in micromolar.

Cytotoxicity of tested compounds in 3T3 cells

Compounds	**IC_{50} (µM)***	**Independent replicates**
JC-01-072	153.1 ± 33.8	4
EA-02-009	106.6 ± 82.3	4
JC-01-074	102.5 ± 8.7	3
JC-01-083	78.2 ± 24.1	4
EA-02-11	43.6 ± 8.3	3

* Mean ± SD. Based on absorbance at 540 nm in MTT assay.

Table 3. Viability of 3T3 cells treated with tested compounds for 24 hours, in microgram per milliliter.

Cytotoxicity of tested compounds in 3T3 cells

Compounds	IC_{50} (µg/ml)*	Independent replicates
JC-01-072	37.6 ± 8.3	4
EA-02-009	34.6 ± 26.7	4
JC-01-074	25.2 ± 2.1	3
JC-01-083	30.9 ± 9.5	4
EA-02-11	10.7 ± 2.0	3

* Mean ± SD. Based on absorbance at 540 nm in MTT assay.

Figures

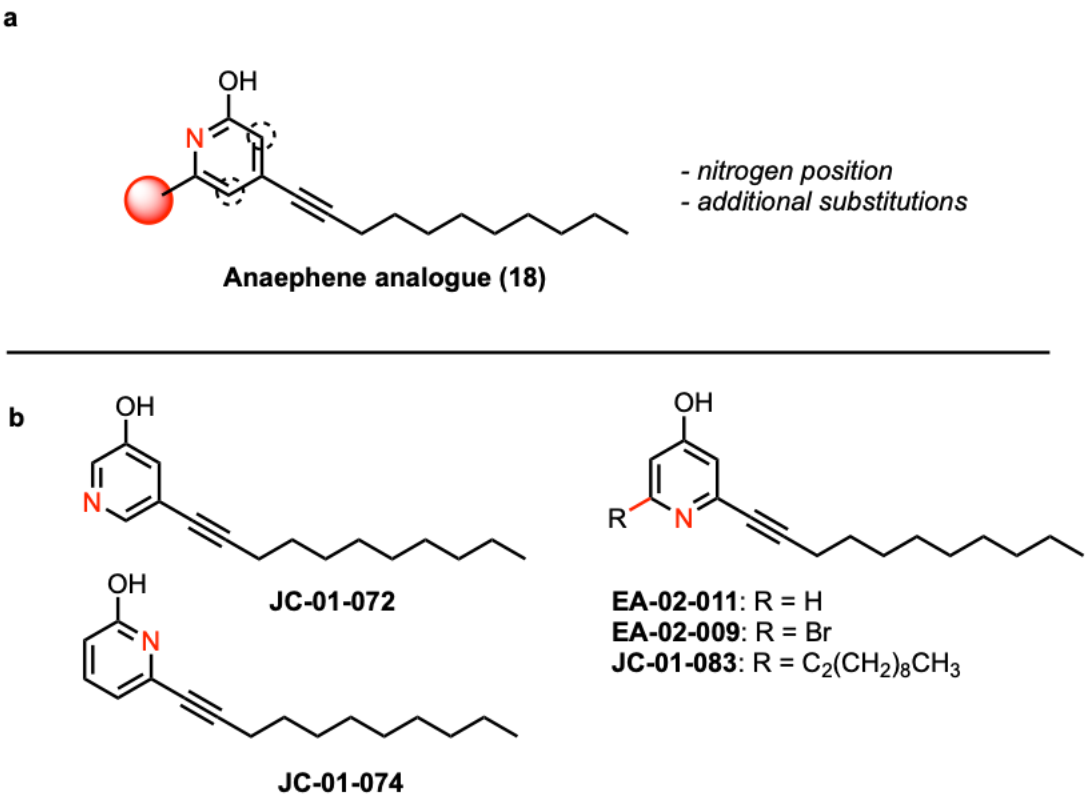

Figure 6: The pyridine analogs and schematic representation of SAR strategy

(a) Strategy for the structure activity relationship study on anaephene analog **18** from previous study.

(b) Target analogs for investigating significance of nitrogen position and additional substitutions to further probe requirements for activity.

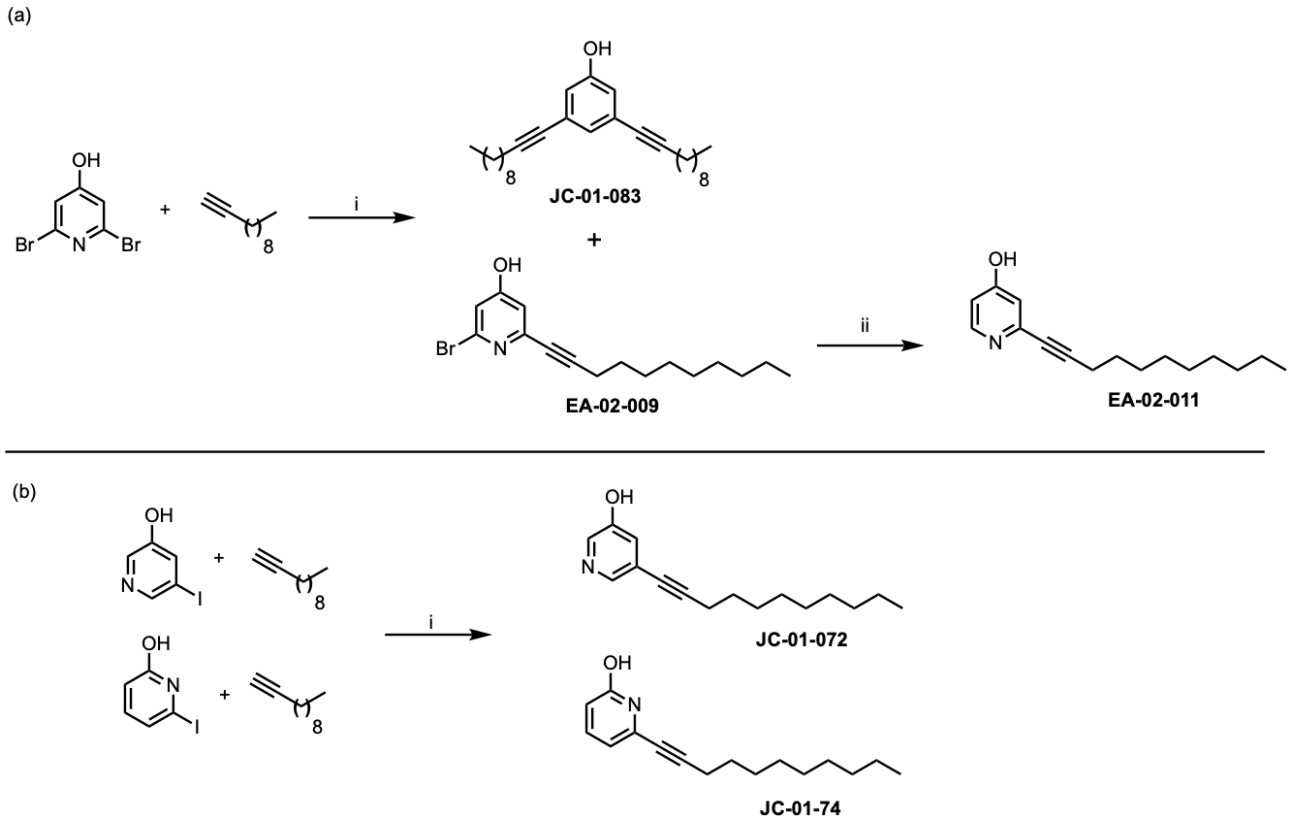

Figure 7: Synthetic strategy used to generate analogs

(a) Analogs JC-01-083 & EA-02-009, were generated in a single reaction (i). (b) Single step synthesis used to generate analogs JC-01-072 & JC-01-074. Reagents and conditions: (i) CuI, Et3N, PdCl2(PPh3)2, MeCN, 24 hr, rt; (ii): n-BuLi, THF, −78°C for 30 min.

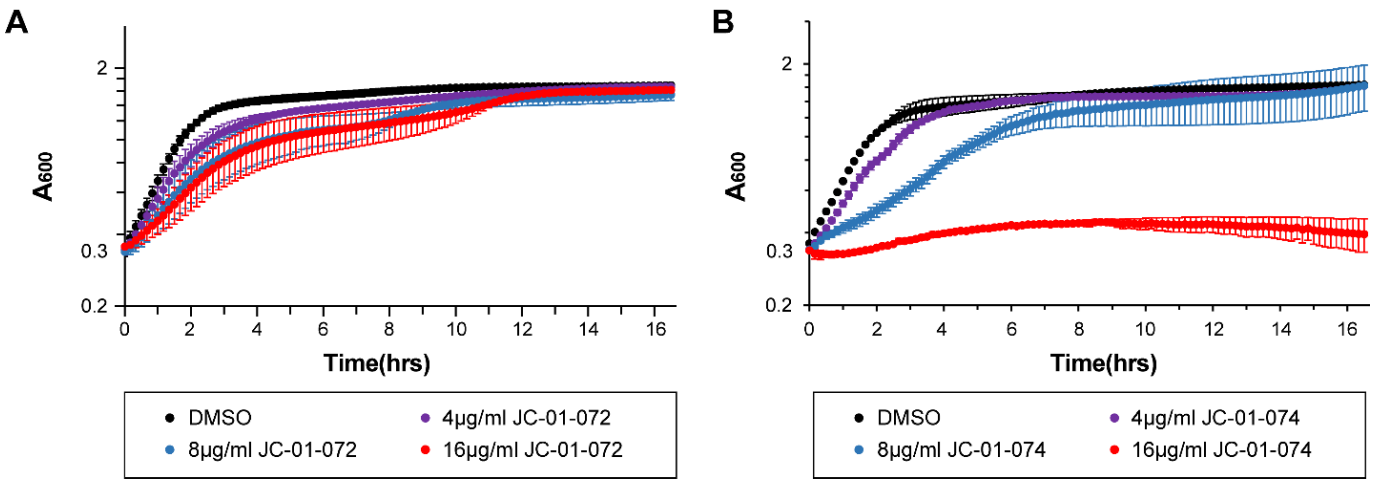

Figure 8: **Growth curves of exponential phase USA 300 LAC**

The impact of alkyl pyridine on exponentially growing USA 300 LAC (OD600nm =0.2-0.3) was assessed by treatment with 4-16µg/ml (A) JC-01-072 and (B) JC-01-072 in two-fold increments in concentration. Optical densities were measured at 600nm at 10-minute intervals for 16-18 hours. (Error bars represent the standard error of mean from three biological replicates).

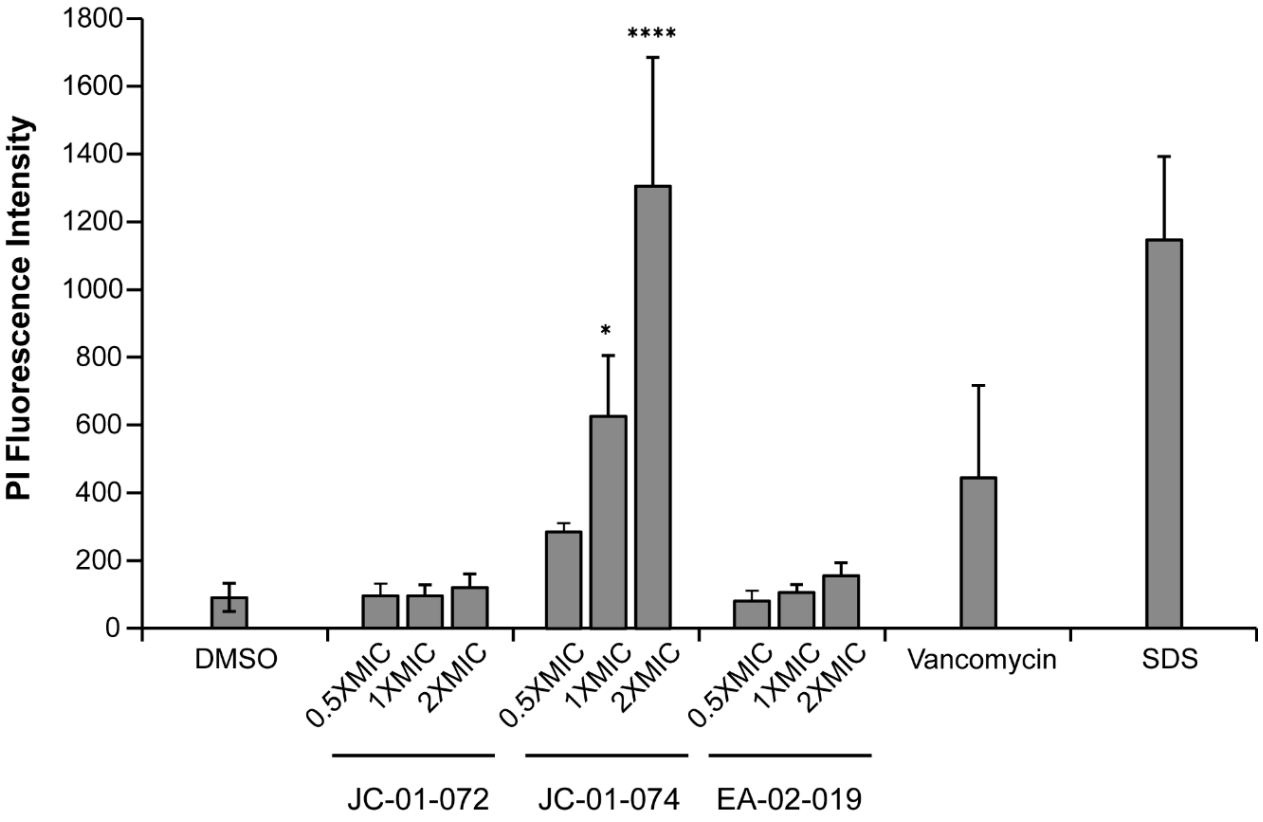

Figure 9: JC-01-074 causes membrane damage in USA 300 LAC

Inner membrane damage was evaluated via propidium iodide (PI) staining. Exponentially growing cultures were exposed to 0.5XMIC to 2X MICs of alkyl pyridine compounds (Table 2) for 60 minutes. Samples treated with DMSO or 4µg/ml vancomycin and 0.25% SDS were included as controls. Cells were collected, washed, resuspended in PBS, and stained with 1µM PI. PI fluorescence measured at 535/615 Ex/Em and normalized to OD600. Error bars represent standard deviation from three biological replicates. One-way ANOVA, Dunnett's multiple-comparison test (* $P<0.05$, **** $P<0.0001$).

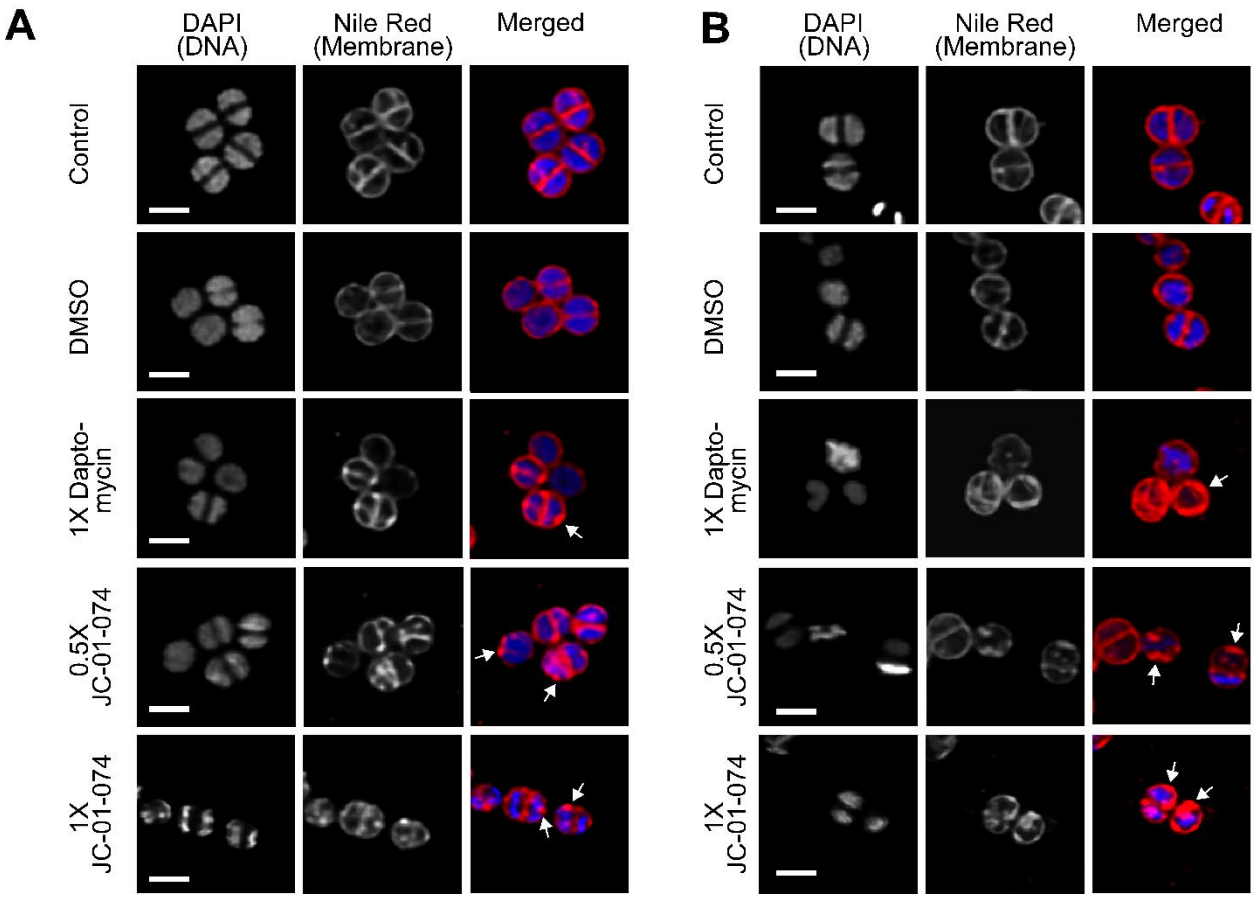

Figure 10: JC-01-074 treatment rapidly induces cell membrane deformations in USA 300 LAC

Exponential phase USA 300 cells in TSB were either left untreated or treated with DMSO, 4µg/ml Daptomycin (1X MIC), 8µg/ml JC-01-074 (0.5X MIC) and 16µg/ml JC-01-074 (1X MIC) for (A)15 minutes and (B) 1 hour under shaking conditions. Cells were collected at indicated time points and stained with DAPI (5µg/ml) and Nile Red (5µg/ml) for 10 minutes, following which cells were imaged on 1% agarose pads. Images are representative of three biological replicates. Scale bar =1.25µm.

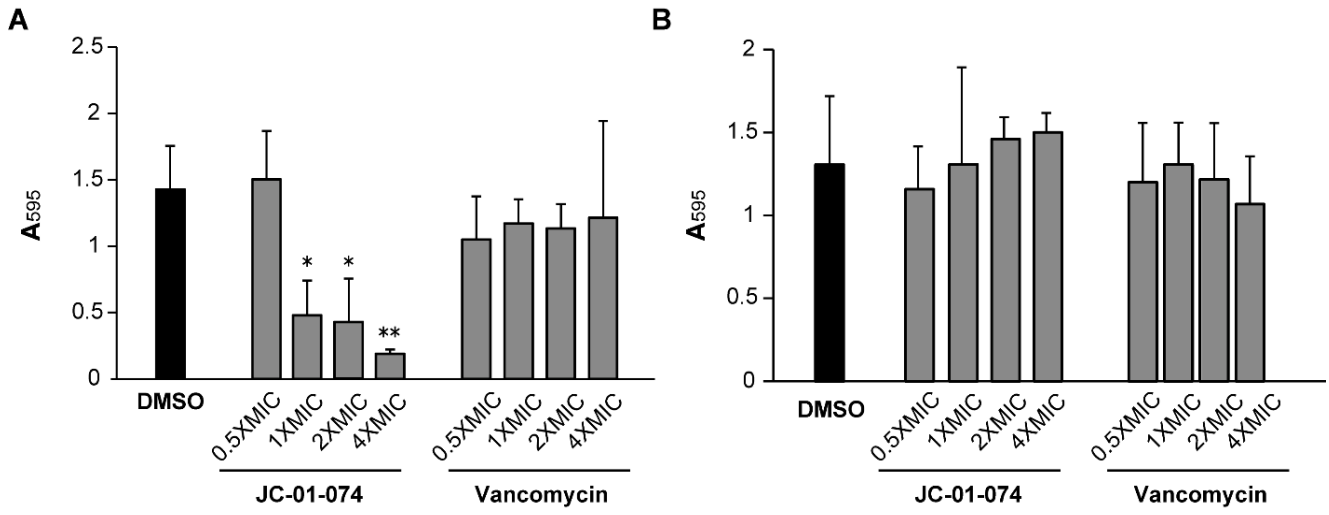

Figure 11: JC-01-074 exerts biofilm inhibitory effects but does not reduce established biofilms

Overnight USA 300 LAC cultures were diluted to an OD600 of 0.001 and incubated until mid-log phase in TSB. (A) For biofilm inhibition assays, cultures were then diluted to an OD 600 of 0.0001 and mixed with JC-01-074 to final concentrations ranging from 0.5MIC to 4X MIC for JC-01-074 and 0.25MIC to 2X MIC for Vancomycin. (B) For biofilm eradication assays, diluted mid-log phase cultures were incubated under static conditions for 24 hours following which planktonic cells were removed. Biofilms were resuspended in TSB supplemented with from 0.5MIC to 4X MIC JC-01-074 and 0.5MIC to 4X MIC Vancomycin and incubated for 24 hours under similar conditions. Biofilm formation was evaluated after 20 hours via crystal violet staining to quantify biofilm (A) accumulation or (B) eradication. Error bars represent standard deviation from three biological replicates. One-way ANOVA, Dunnett's multiple-comparison test (* $P<0.05$, ** $P<0.01$).

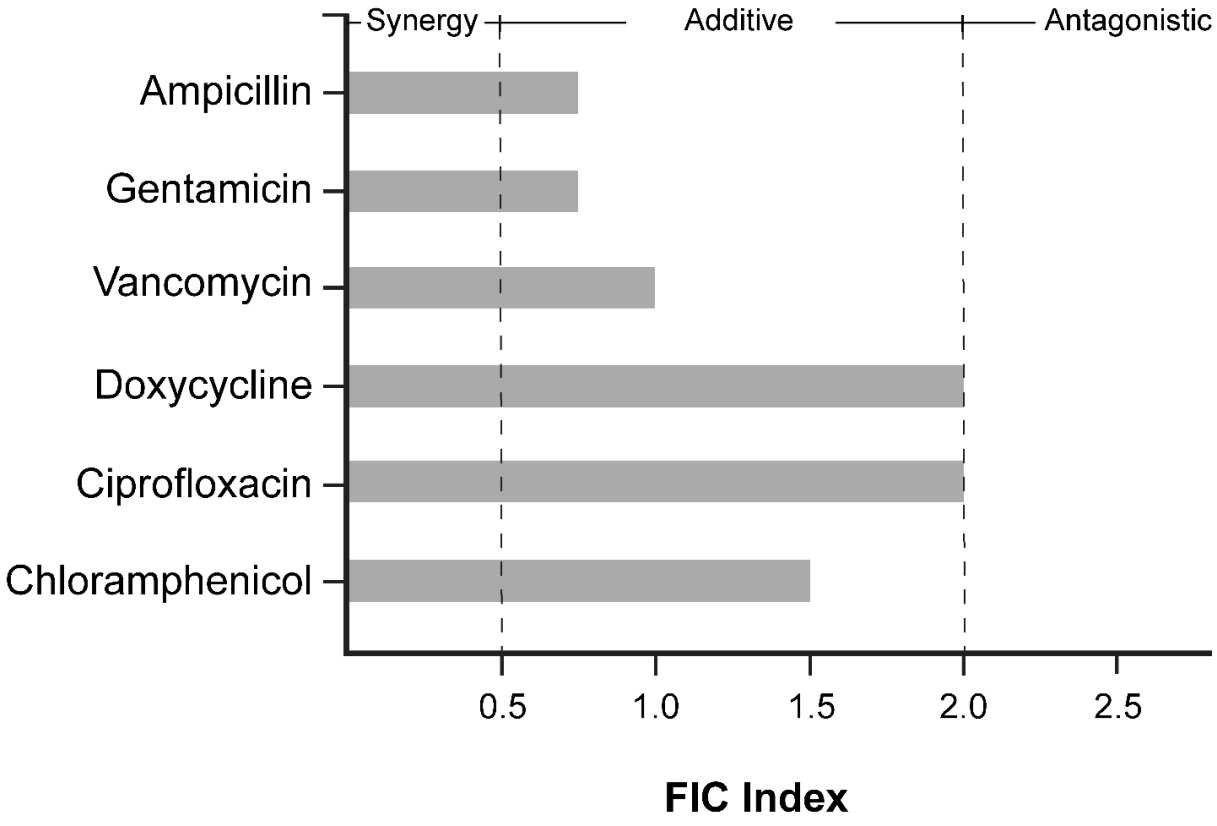

Figure 12: Synergy (FIC index) of JC-01-074

FIC index (sum of FICs) of JC-01-074 tested in combination with ampicillin, gentamicin, ciprofloxacin, doxycycline, vancomycin, and chloramphenicol. FICs were calculated as the ratio of the MIC of the antimicrobial in combination over the MIC of the antimicrobial alone. Sum of FIC or FICi was calculated as the sum of the FICs of the antimicrobials tested in combination. Interactions were categorized as synergistic (<0.5), additive (<1), No interaction (<2) and antagonistic (>2). Checkerboard results were from two biological replicates.

Conclusion

What started off as a small project to report on the synthesis of two biologically active natural products, now is a large study, going on five years, with collaborations with microbiologist and cell biologists. I first worked on the Anaepehene project as an undergraduate student. We did not expect it to get this far, however very interesting analogues that warranted more investigation where found. Through SAR studies and biological assessments, we were able to modify and further develop the Anaepehene molecular template and obtain potent and highly interesting molecules with desirable biological activities for drug development candidacy.

It has been an absolute honor to work on this project for nearly five years now, however I must announce that I will be pursuing other endeavors to advance my career. The next directions with the Anaephene project would be to take the lead alkylpyridine analogues and asses them further with various in vitro/PK studies to determine candidacy for in vivo studies. It would be so great to know that someone will be continuing these efforts with the appropriate next steps, that will remain uncertain, as the direction of my career does not align with this research. I am excited for the future, hopefully this work will, one day, help scientist develop more antibiotics. Just maybe the Anaepehene molecular template and the analogs I have generated may be of use and contribute to the efforts of replenishing our antibiotic defenses against deadly bacteria infections.

I'd like to conclude by thanking everyone involved in this study. Thank you, Dr. Mills, for allowing me the pleasure of working on this project it has been incredibly challenging,

rewarding and fun. Thank you, David, for mentoring me and helping me be a better chemist. Thank you, Emmanuel, for all of your help with my work you are a great colleague and a better friend! Lastly, I'd like to thank Martin Engelke, Ayoola Fasawe, Gracious Donkor, Jan Dahl and Patrick Tawiah for making the biological assessments possible. Thank you all for all your help and support.

Supplementary Figures

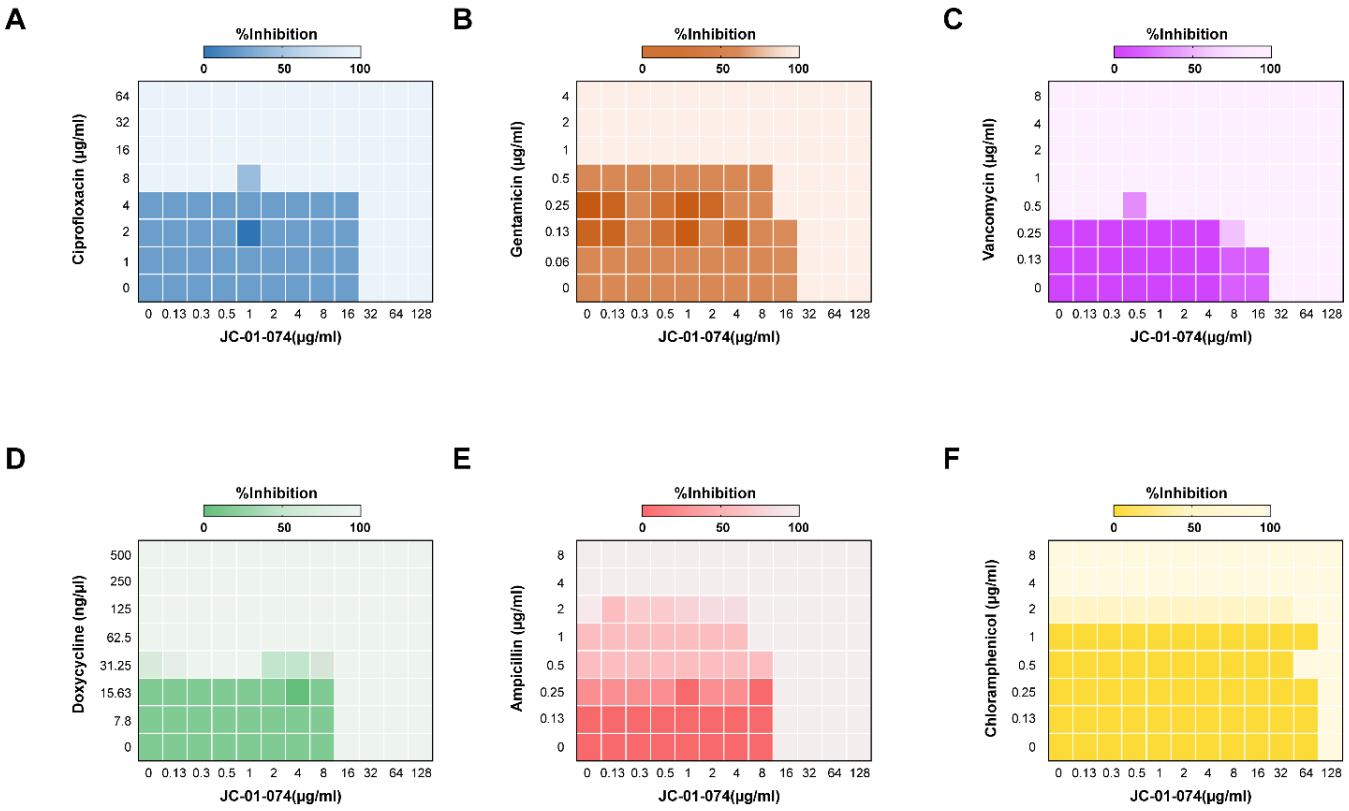

S1. Checkerboard assays with JC-01-074

JC-01-074 tested in combination with ampicillin, gentamicin, ciprofloxacin, doxycycline, vancomycin, and chloramphenicol against USA 300 LAC to determine if JC-01-074 had synergistic effects in combination with conventional antibiotics. FICs were calculated as the ratio of the MIC of the antimicrobial in combination over the MIC of the antimicrobial alone. Antibiotics tested in combination were initially serially diluted two-fold in MHB on a longitudinal axis in a polystyrene 96 well plate. JC-01-074 was then serially diluted two-fold across the 96 well plate horizontal axis.

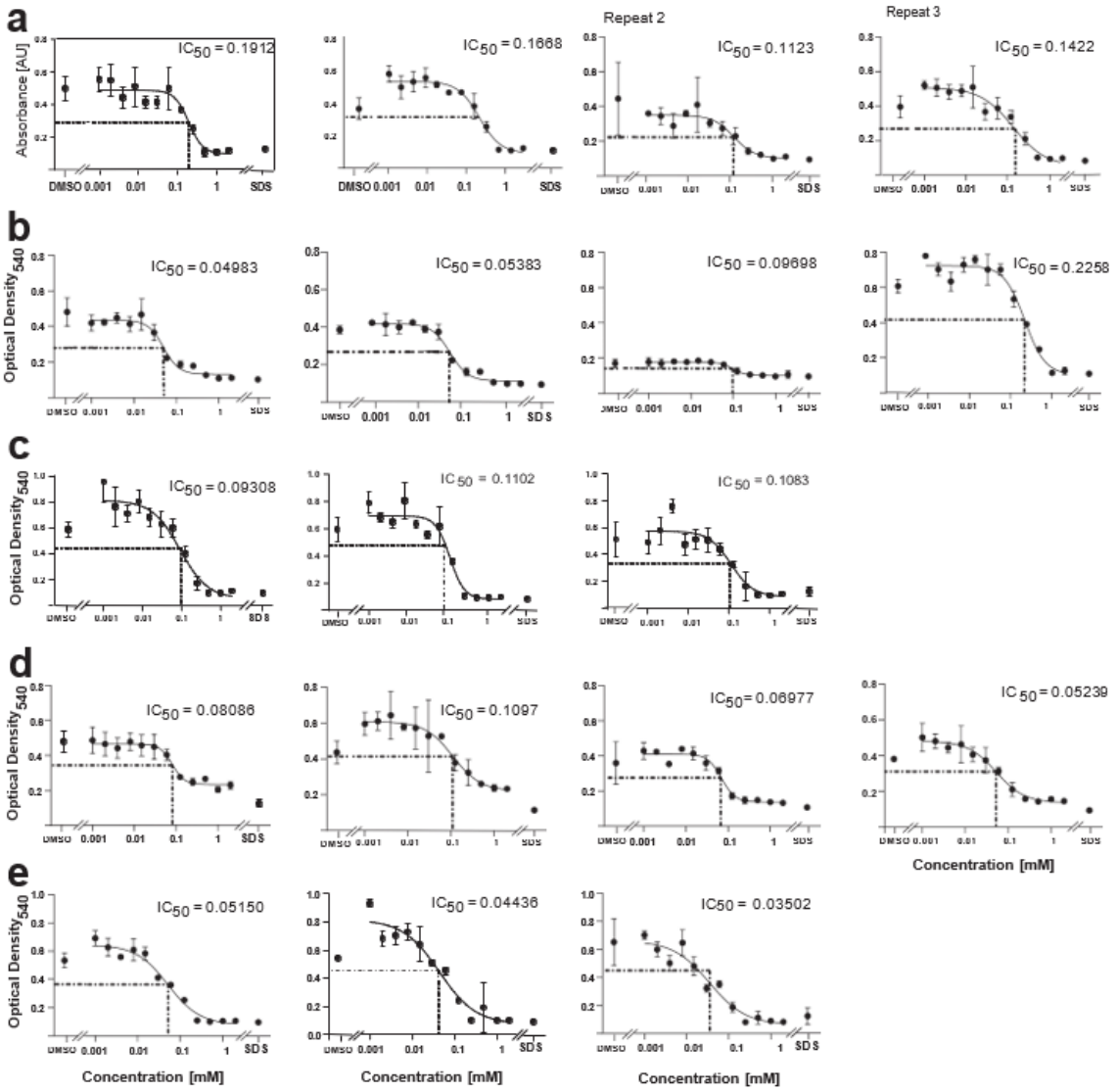

S2. IC50 curves from MTT assay

Viability of 3T3 cells treated with tested compounds for 24 hours. Cells were treated with different concentrations of the indicated compounds for 24 hours and then cell viability was assessed with an MTT assay. Treatment with 1% SDS in medium (SDS) and 2% DMSO in medium (DMSO), served as cell death and vehicle control, respectively. Graphs show the mean absorbance at 540 nm of MTT

containing cell supernatant of cells treated with compound JC-01-72 (**a**), EA-02-09 (**b**), JC-01-74 (**c**), JC-01-83 (**d**), EA-02-11 (**e**). Averages are derived from three dependent data points (triplicates on plate) from 3-4 independent experiments. Controls were carried out in 6 dependent replicates per plate. Error bars, SEM.

Supporting information (characterization)

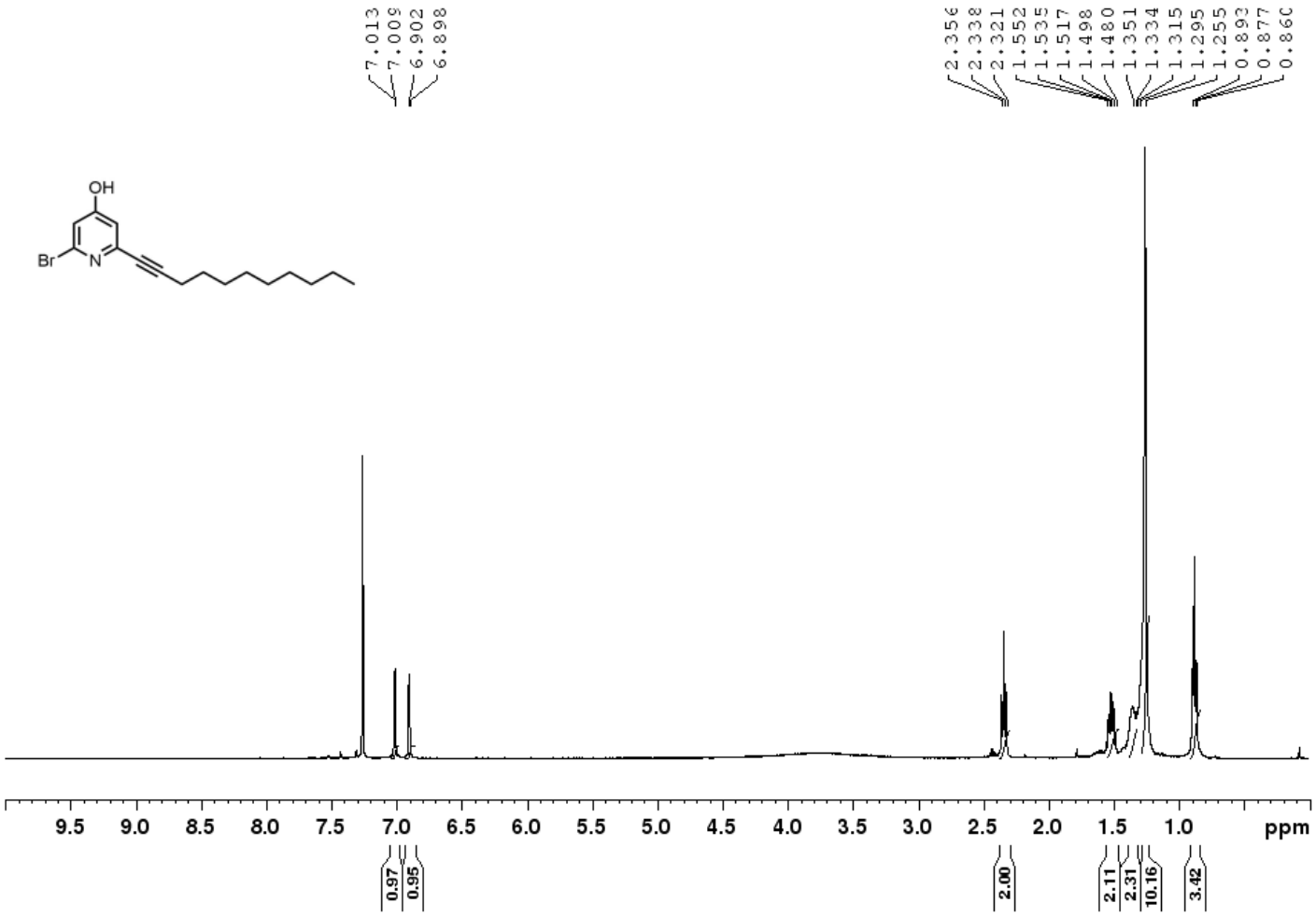

Figure S3. ^{1}H NMR spectrum of **EA-02-009** in $CDCl_3$.

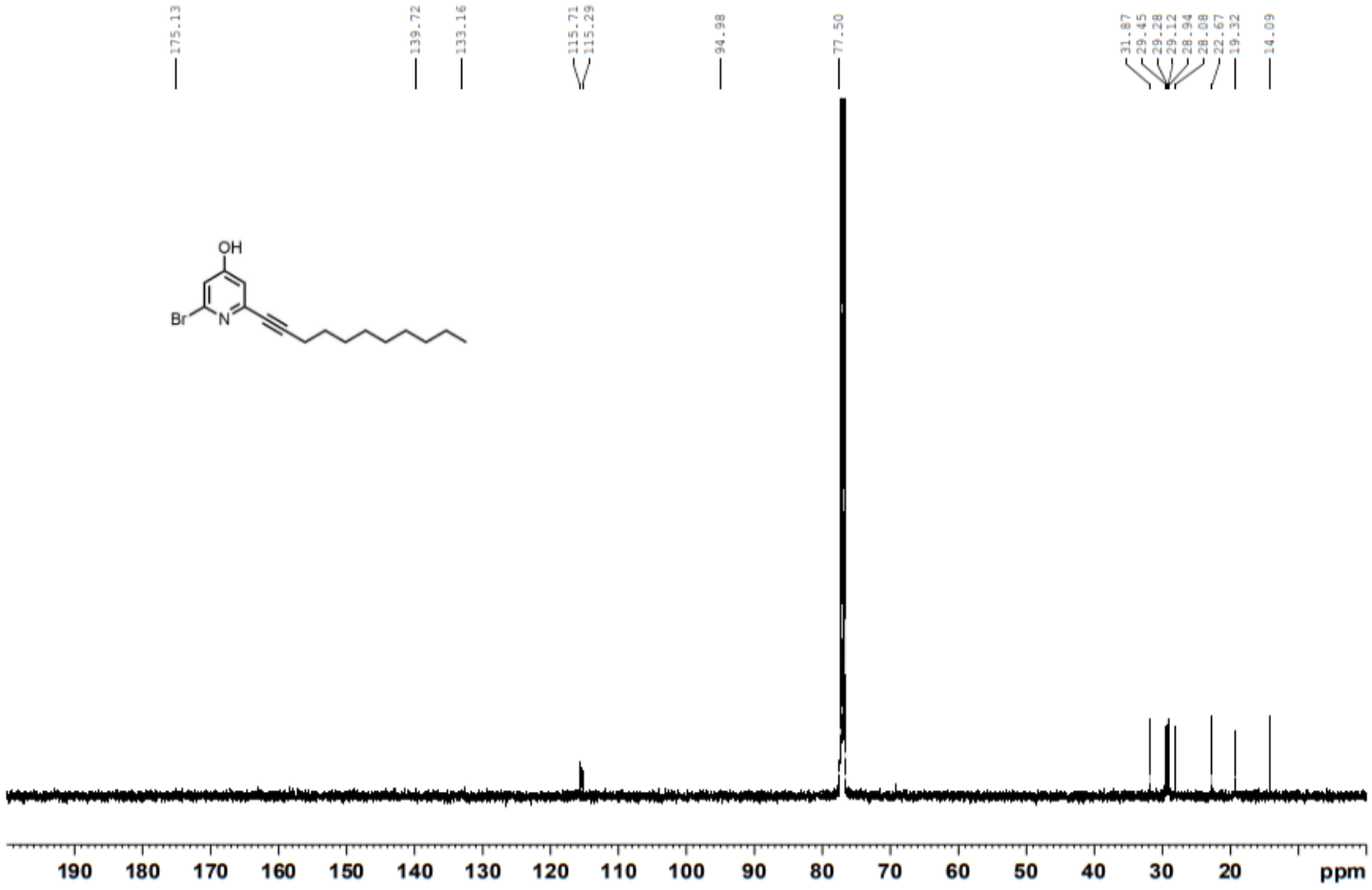

Figure S4. ^{13}C NMR spectrum of **EA-02-009** in $CDCl_3$.

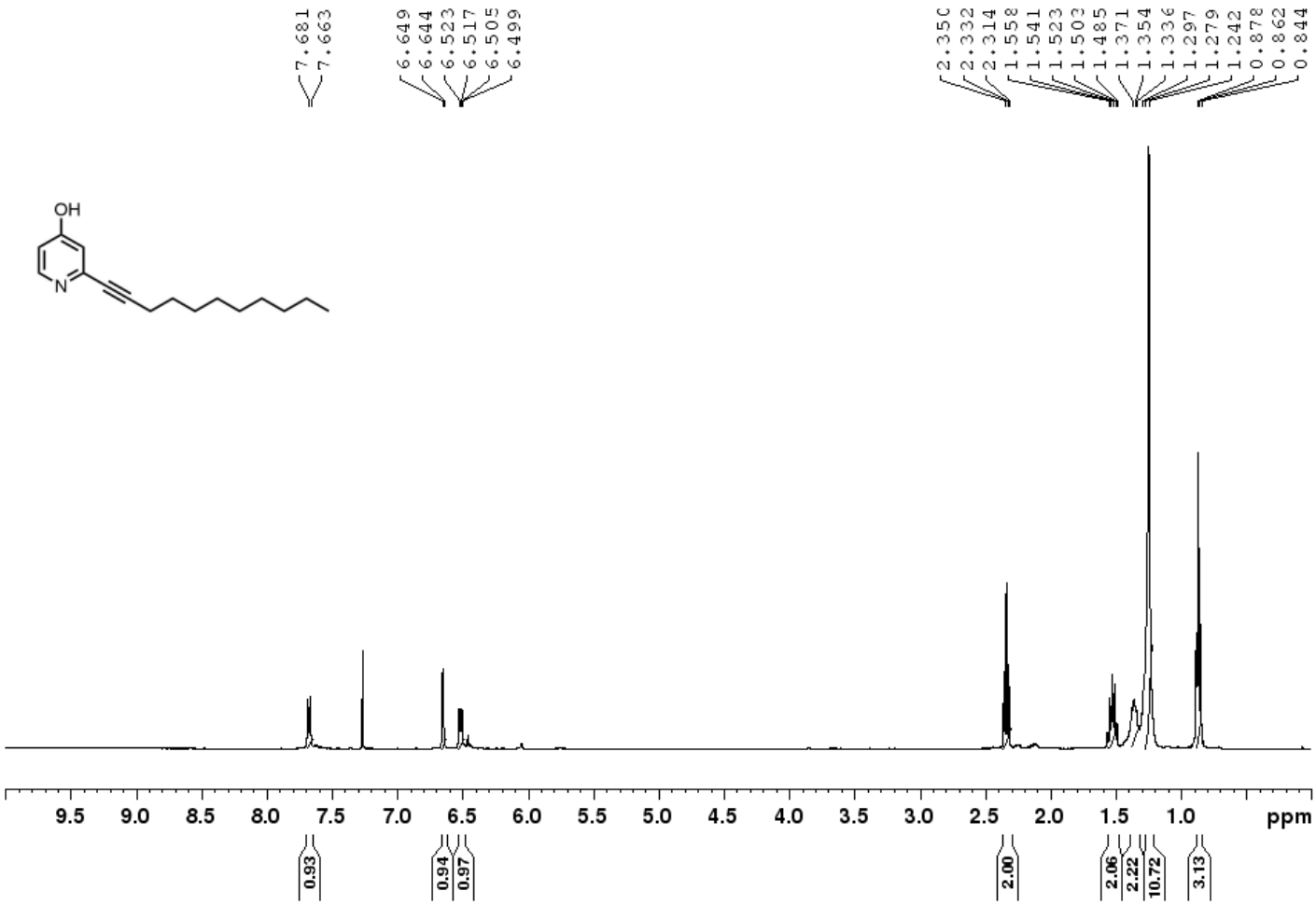

Figure S5. ^{1}H NMR spectrum of **EA-02-011** in $CDCl_3$.

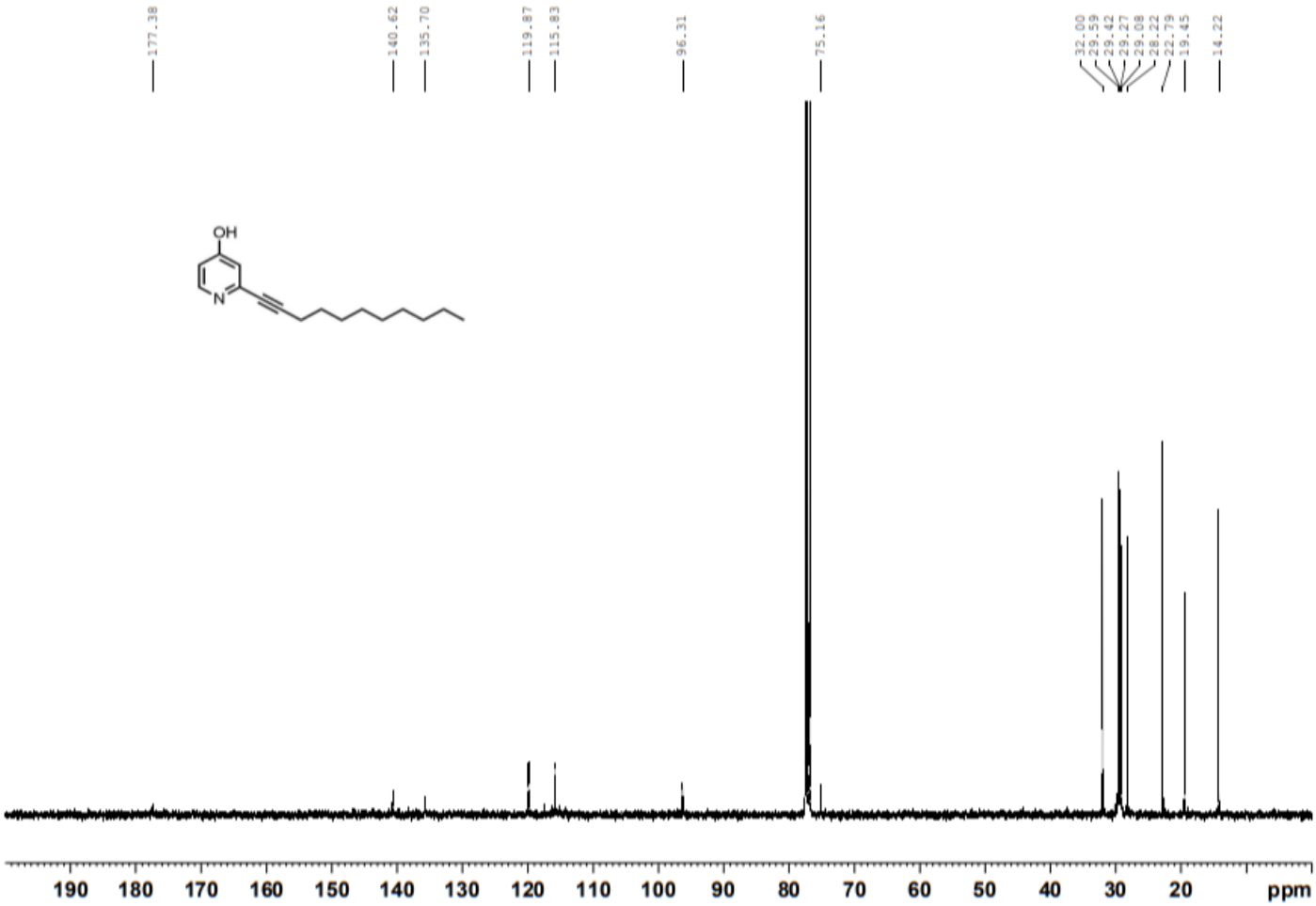

Figure S6. ^{13}C NMR spectrum of **EA-02-011** in $CDCl_3$.

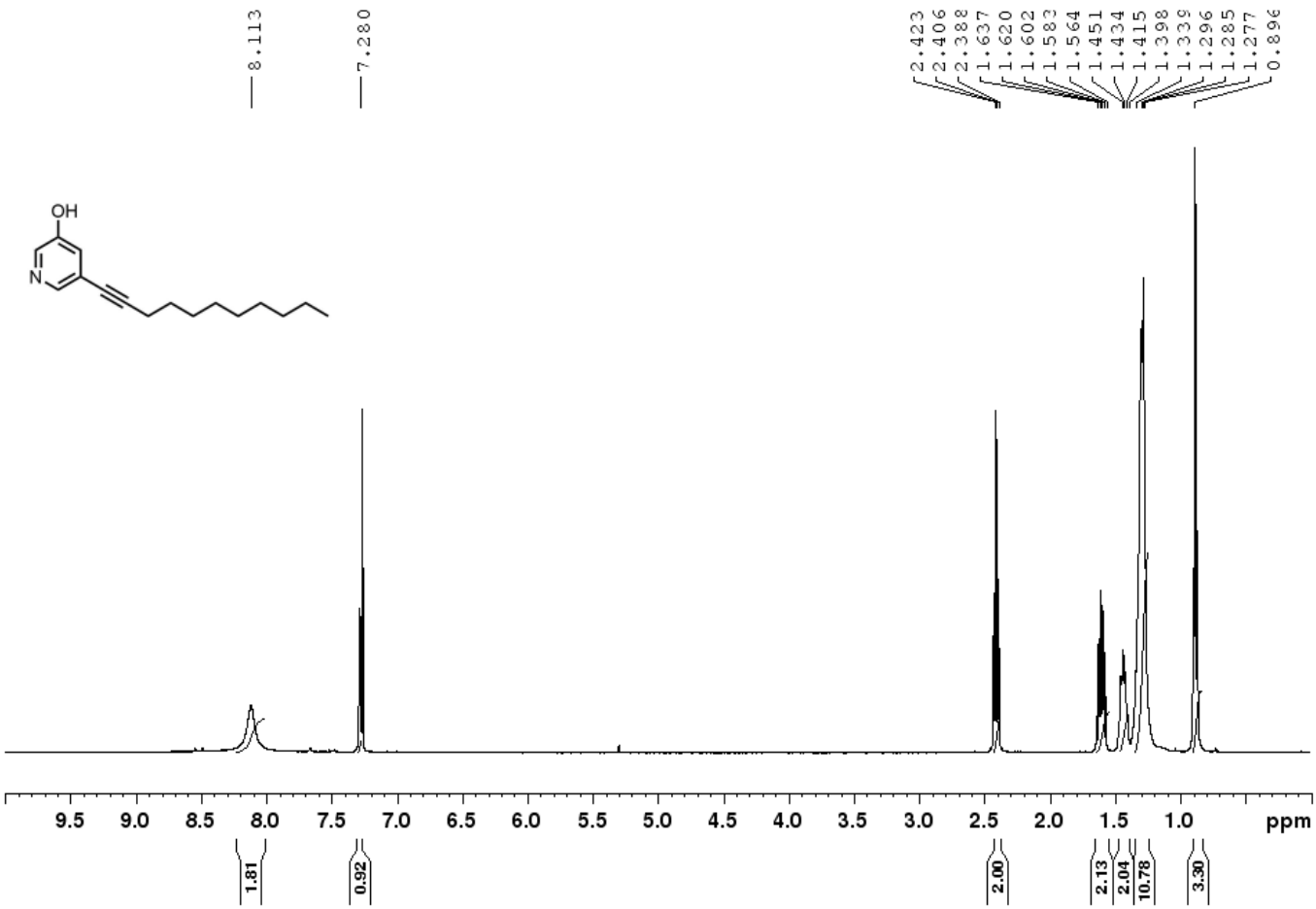

Figure S7. ^{1}H NMR spectrum of **JC-01-072** in $CDCl_3$.

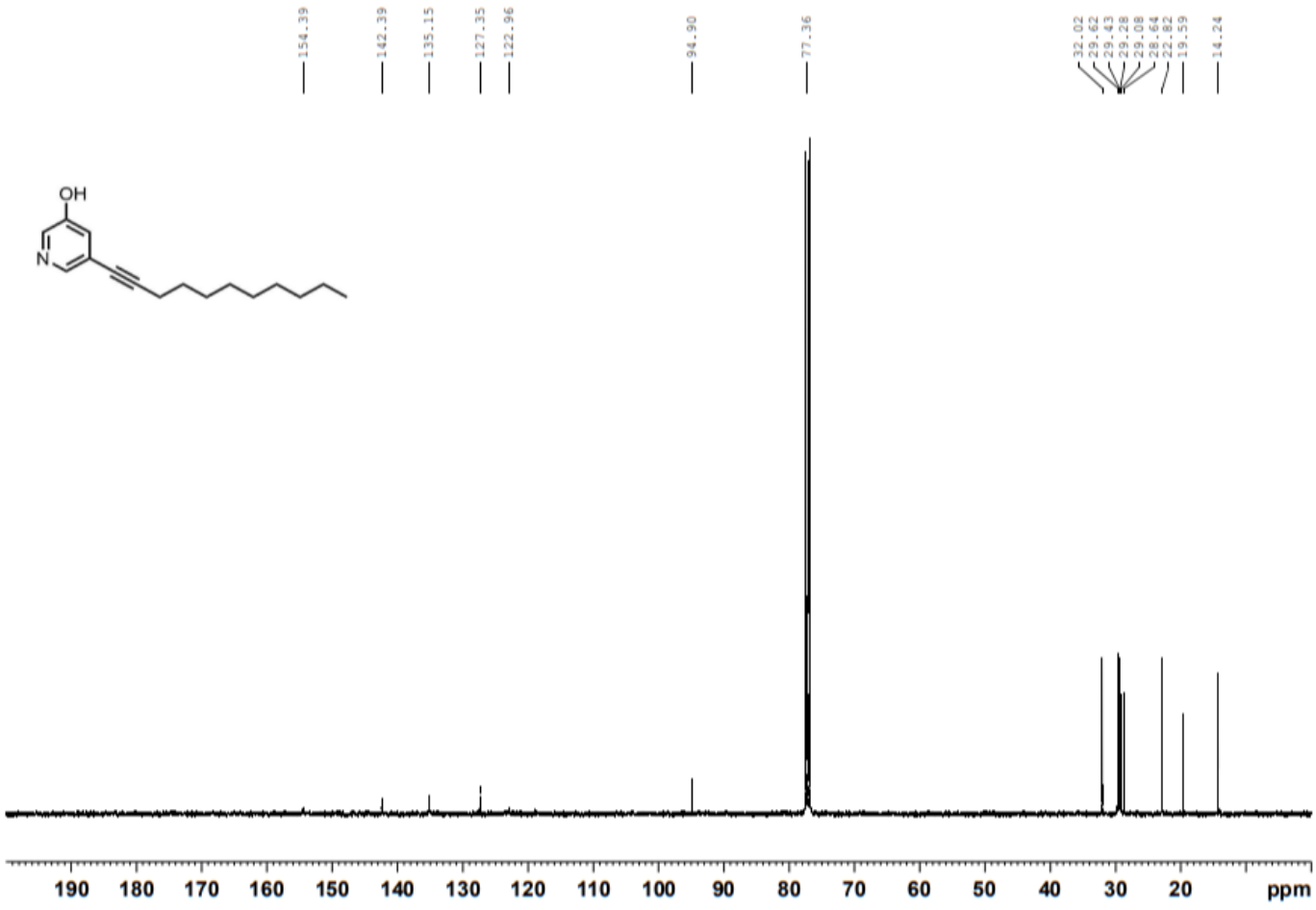

Figure S8. ^{13}C NMR spectrum of **JC-01-072** in $CDCl_3$.

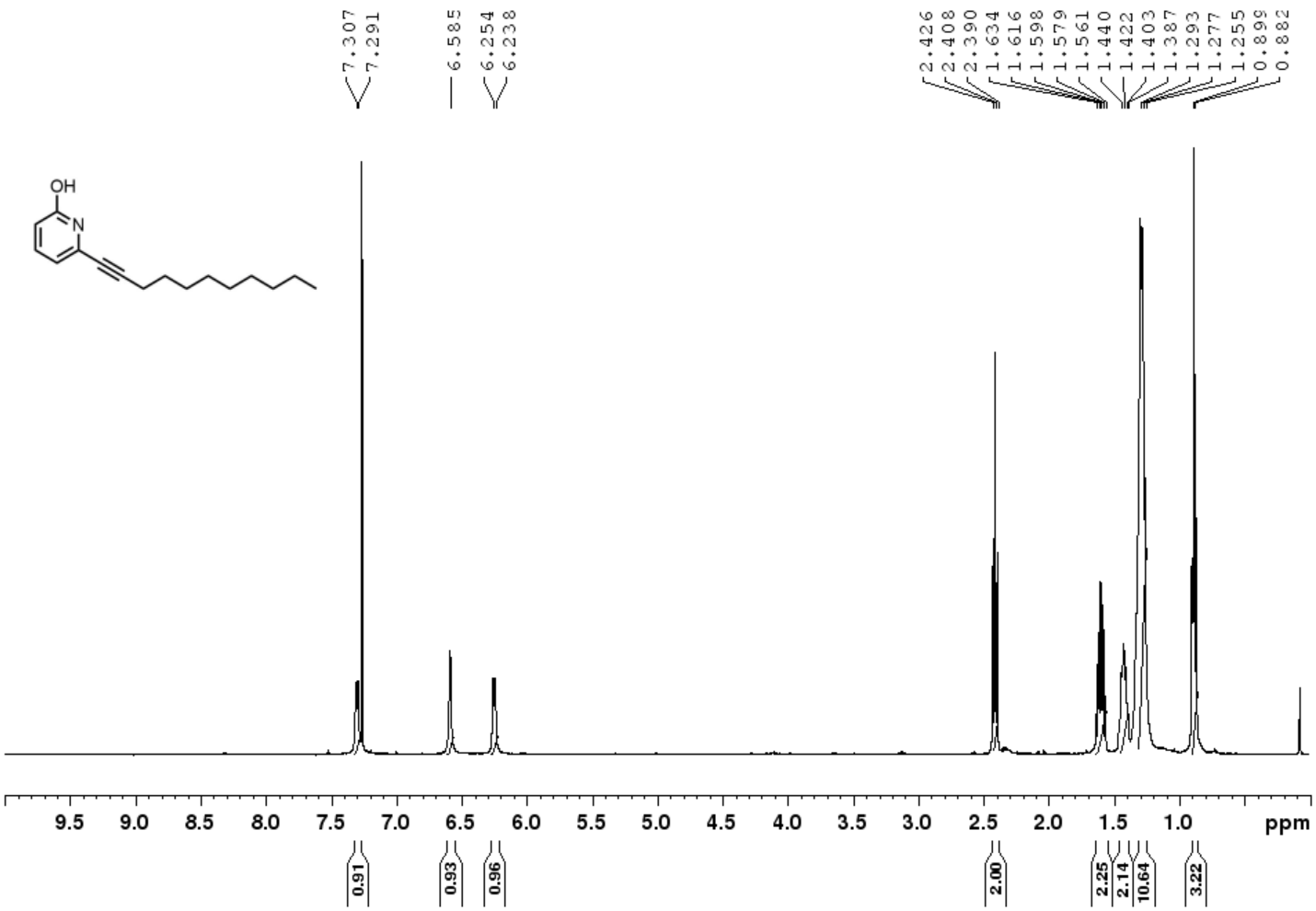

Figure S9. ^{1}H NMR spectrum of **JC-01-074** in $CDCl_3$.

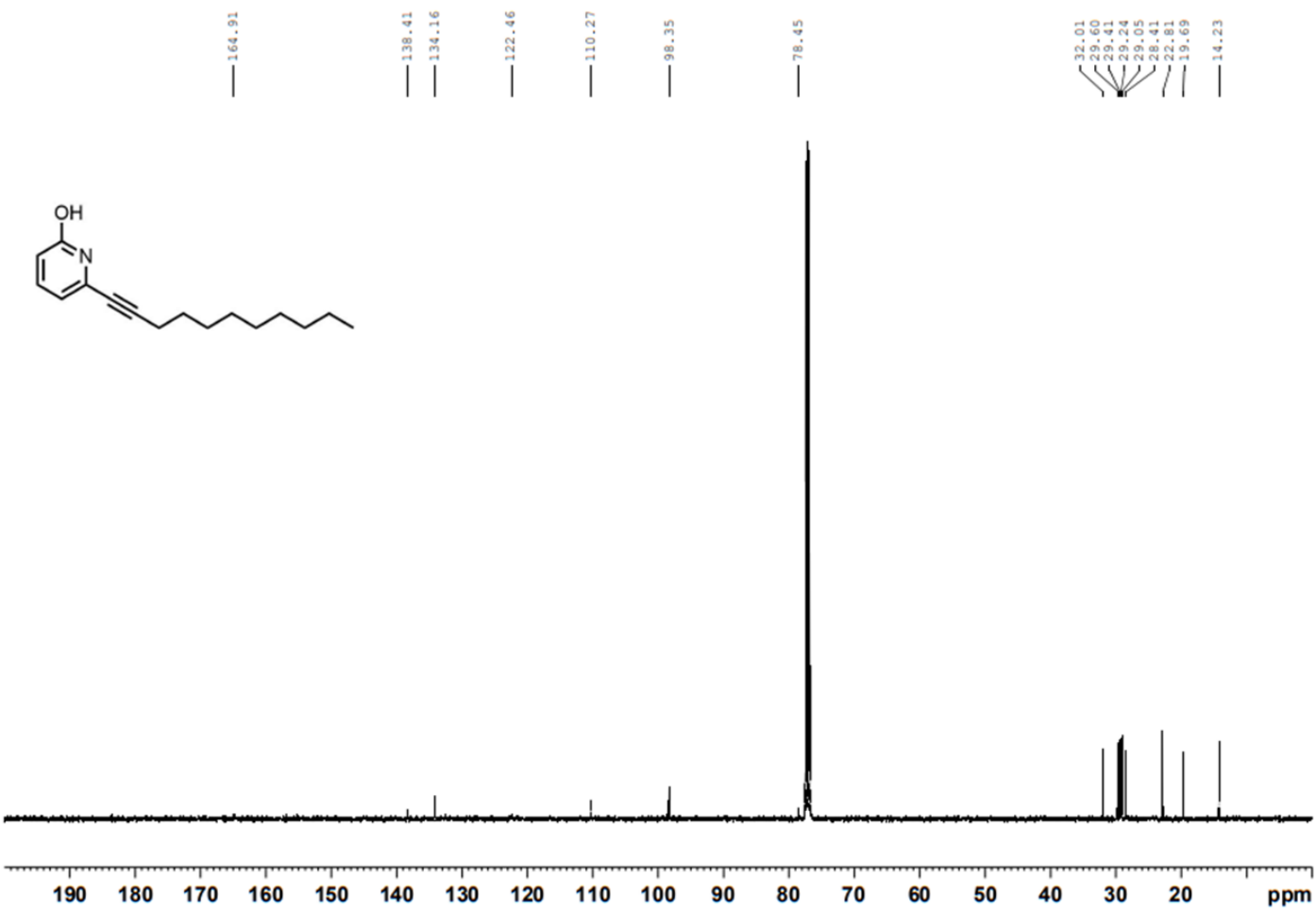

Figure S10. ^{13}C NMR spectrum of **JC-01-074** in $CDCl_3$.

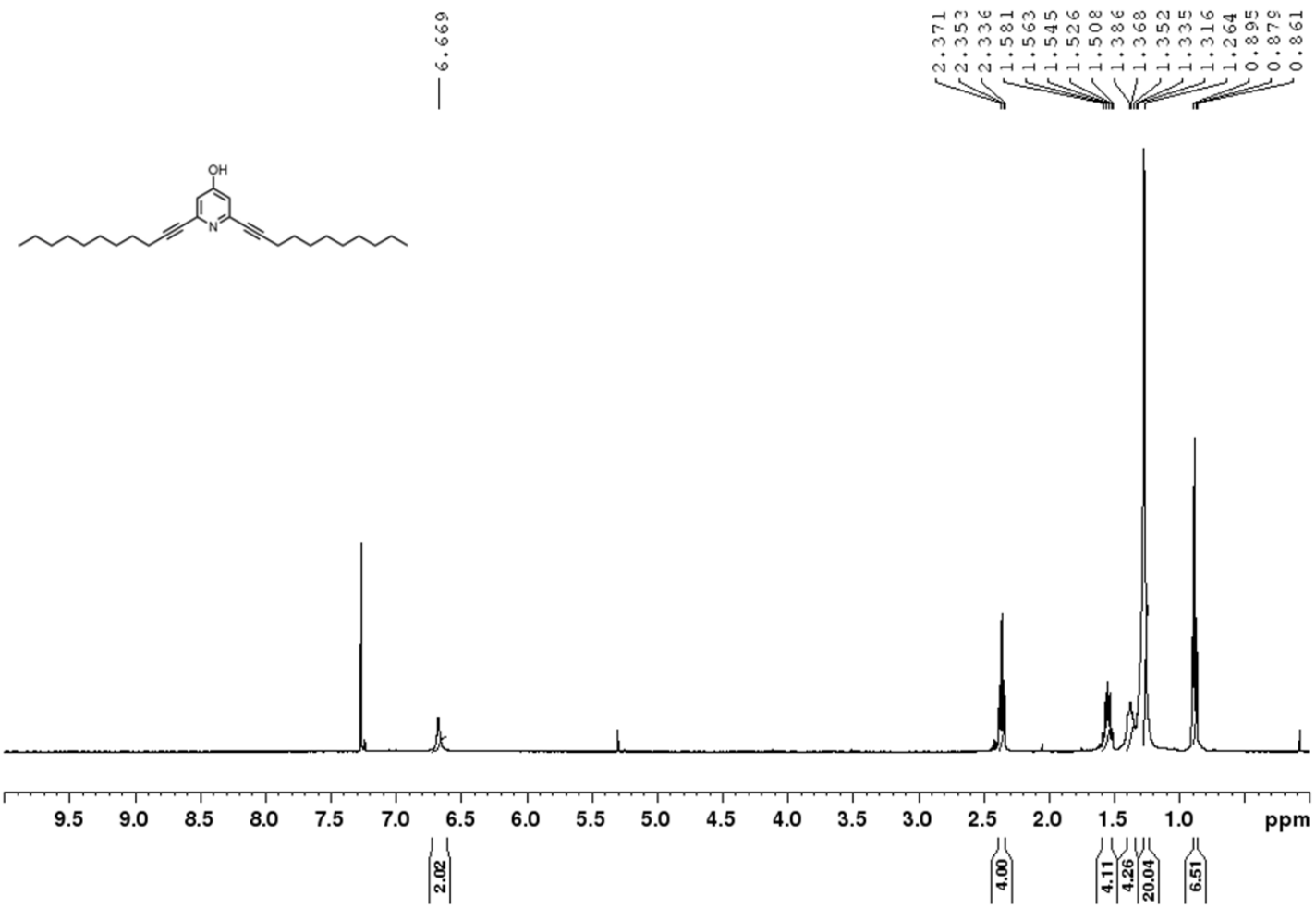

Figure S11. ^{1}H NMR spectrum of **JC-01-083** in $CDCl_3$.

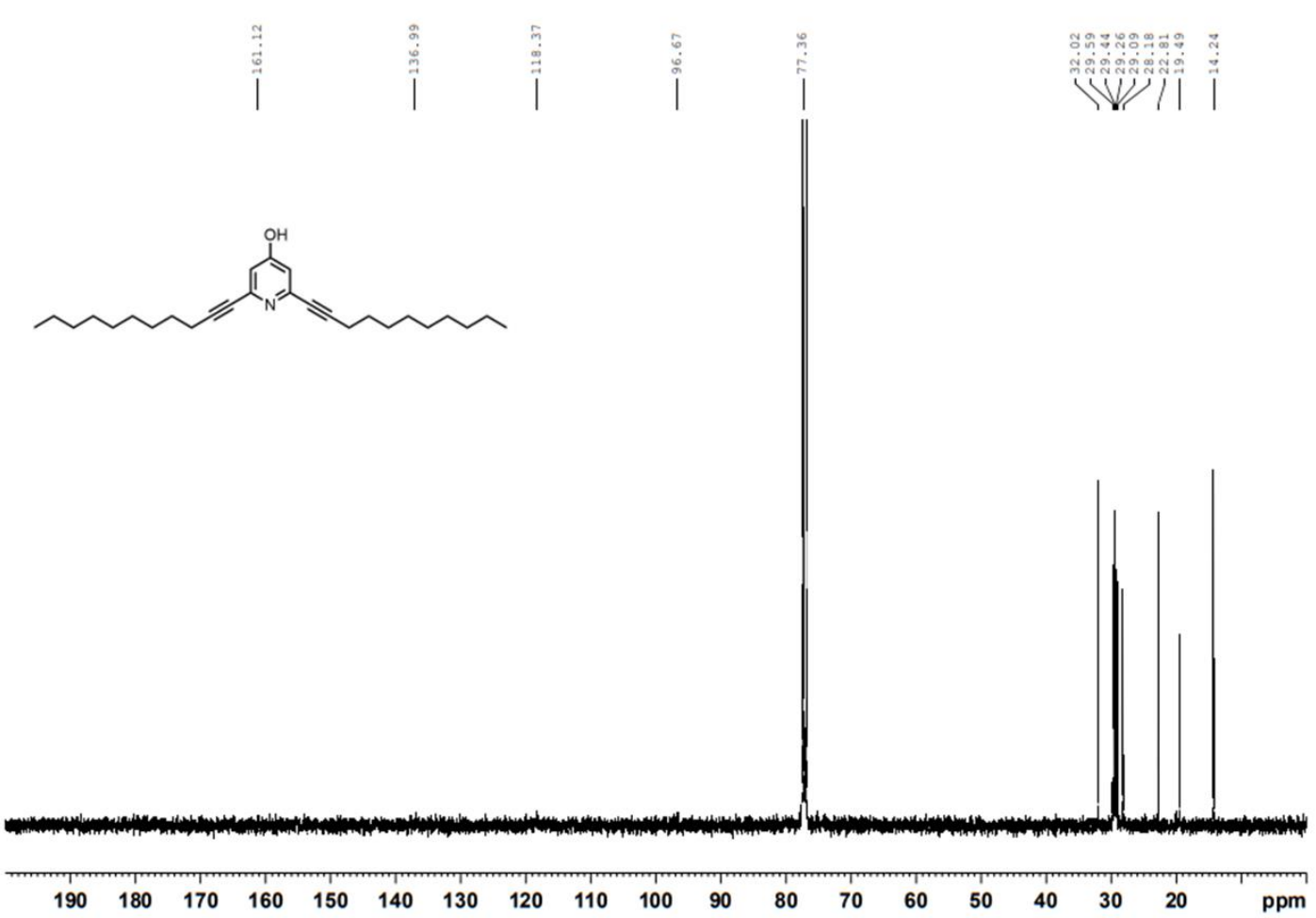

Figure S12. ^{13}C NMR spectrum of **JC-01-083** in $CDCl_3$.